Electronic Supporting Information

Synthesis, Structure, Self-assembly and Genotoxicity Evaluation of a Series of Mn-Anderson Cluster based Polyoxometalate-organic Hybrids

V. S. V. Satyanarayana,[a‡] Pulikanti Guruprasad Reddy[a‡] and Chullikkattil P. Pradeep[a]*

[a] School of Basic Sciences, Indian Institute of Technology Mandi, Mandi - 175001, Himachal Pradesh, India.

E-mail: pradeep@iitmandi.ac.in; Fax: (+91)1905 267 009.

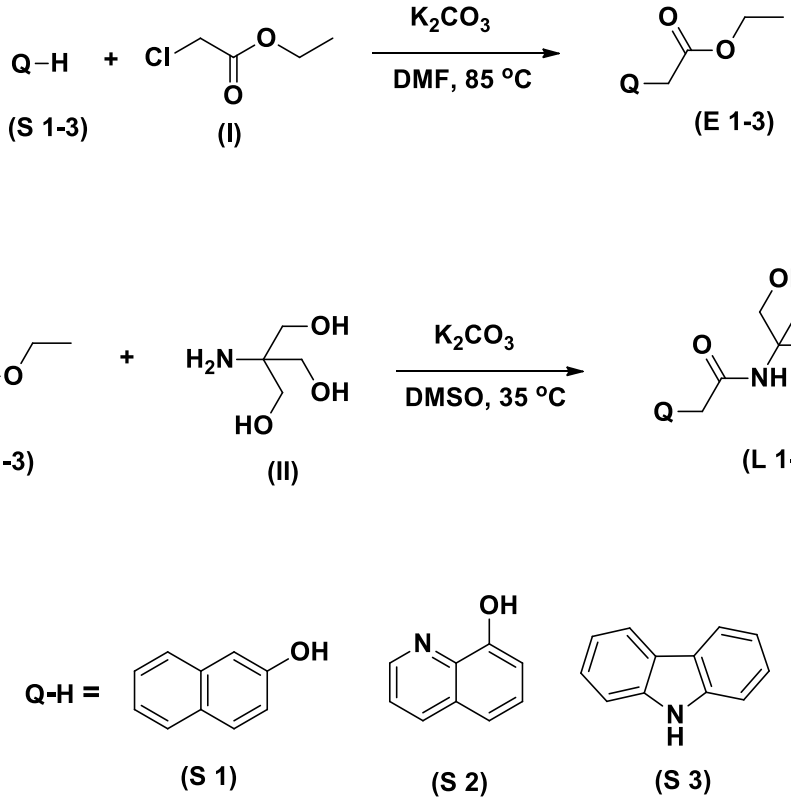

Scheme S1. Synthetic protocol of ligands **L1-L3**

EXPERIMENTAL SECTION

Materials and methods

All the chemicals and solvents were purchased from commercial sources and used as received. Acetonitrile (CH_3CN) was dried using calcium hydride (CaH_2) and dimethyl sulfoxide (DMSO, HPLC grade) was dried using molecular sieves (4 Å x 1.5 mm). 2-Naphthol, 8-hydroxy quinoline and 9 *H*-carbazole were purchased from Sigma Aldrich. Tetrabutylammoniumoctamolybdate, $TBA_4[Mo_8O_{26}]$, was prepared by following a literature procedure.[1] FT-IR spectra were recorded on a Perkin Elmer Spectrum 2 spectrophotometer using KBr pellets. ^1H and ^{13}C NMR spectra were recorded on Jeol JNM ECX 500 MHz spectrometer in DMSO-d_6. TGA measurements were performed on NETZSCH STA 449 F1 JUPITER Series instrument. The heating rate employed was 10 ºC/min under N_2 atmosphere over a temperature range of 25-1000 ºC. ESI-MS spectra of compounds were recorded on Bruker HD compact instrument. The chromosomal aberrations were analyzed by using Nikon Eclipse LV100 POL optical microscope at 100X. Confocal images were taken on NIKON eclipse TI inverted microscope at 60X (oil merging) using TRITC, FITC and Cy-5 lasers. Dynamic light scattering studies were conducted on Malvern, Zetasizer instrument. Transmission Electron Microscope (TEM) analyses of hybrids **M1-M3** were conducted on FEI TECNAI F 20 HRTEM instrument operating at an accelerating voltage of 120 KV and FEI Morgagani 268 instruments.

X-ray crystallography

Single crystal X-ray data were collected on Agilent SuperNova diffractometer, equipped with multilayer optics monochromated dual source (Cu and Mo) and Eos CCD detector, using Mo-Kα (0.71073 Å) radiation at temperature 150 K. Data acquisition, reduction and analytical face-index based absorption correction were done using the program CrysAlisPRO.[2] The structure was solved with ShelXS[3] and refined on F^2 by full matrix least-squares techniques using ShelXL[3] in Olex[2] (v.1.2) program package.[4] Anisotropic displacement parameters were applied for all the atoms, except hydrogen atoms and some less intensely scattered carbon and nitrogen atoms. H atoms were calculated into their positions or located from the electron density map and refined as riding atoms using isotropic displacement parameters.

The solvents present in the structure of **M2** was found to be highly disordered, so the SQUEEZE procedure of the PLATON program[5] was used, which suggested 316 electrons per unit cell. Before the use of SQUEEZE, the solvents present in the asymmetric unit resembled two molecules of dimethylformamide (DMF). The crystal was grown from DMF solvent as well. One molecule of DMF contains 40 electrons. Therefore, the 316 electrons suggested by SQUEEZE is close to the electron density required for 8 DMF molecules (320). So the contents of the unit cell were adjusted accordingly. 8 DMF molecules per unit cell correspond

to 2 DMF molecules per cluster hybrid. The crystal and structure refinement data for **M1** and **M2** are summarized in Table S4.

CCDC 1061758 (**M1**) and1061759 (**M2**) contain the supplementary crystallographic data for this paper. These data can be obtained free of charge from The Cambridge Crystallographic Data Centre *via*www.ccdc.cam.ac.uk/data_request/cifdata.

General procedure for the synthesis of E1-E3

Esters **E1-E3** were synthesized according to the literature procedure.[6-9] In 40 mL of dry DMF, starting material (**S1**, **S2** or **S3,** see Scheme S1) and potassium carbonate (K_2CO_3) were stirred for 15 min. Ethyl chloroacetate was added to the above reaction mixture and stirred again for 24 hours at 85 ºC under nitrogen atmosphere. After completion, the reaction mixture was poured into crushed ice and stirred for 10 min. The precipitated solid was separated by filtration, washed with excess of water and dried under vacuum.

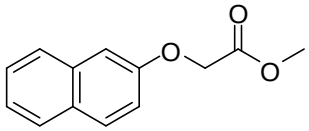

E1

*Ethyl 2-(naphthalen-2-yloxy)acetate, **E1***

The general procedure as above was followed using **S1** (6.0 g, 41.64 mmol), K_2CO_3 (11.51 g, 83.29 mmol) and ethyl chloroacetate (5.08 g, 41.64 mmol) to get the compound **E1**. FT-IR: ν_{max}/cm^{-1} 2981 (ν CH_3), 2908 (ν CH_2), 1761 (ν C=O), 1627-1596 (ν C=C), 1206-1182-1078 (ν C-O), 834-742 (ν C-H) cm^{-1}.

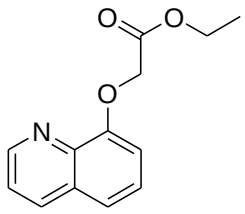

E2

*Ethyl 2-(quinoline-8-yloxy)acetate, **E2***

The general procedure as above was followed using **S2** (6.0 g, 41.36 mmol), K_2CO_3 (11.43 g, 82.72 mmol) and ethyl chloroacetate (5.04 g, 41.36 mmol) to get the compound **E2**. FT-IR:

ν_{max}/cm^{-1} 2993 (ν CH_3), 1749 (ν C=O), 1670, 1505-1450 (ν C=C), 1377, 1322, 1224, 1121 (ν C-O), 1084, 1011, 828 (ν C-H) cm^{-1}.

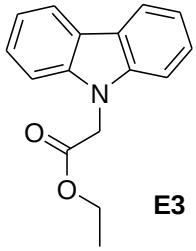

E3

*Ethyl 2-(9H-carbazole-9-yl)acetate, **E3***

The general procedure as above was followed using **S3** (6.0 g, 35.88 mmol), K_2CO_3 (9.9 g, 71.76mmol) and ethyl chloroacetate (4.3 g, 35.88 mmol) to get the compound **E3**. FT-IR: ν_{max}/cm^{-1}2987 (ν CH_3), 1932, 1889, 1737 (ν C=O), 1602-1450 (ν C=C), 1328-1224 (ν C-O), 998, 1029, 848-748 (ν C-H) cm^{-1}.

General procedure for the synthesis of L1-L3

In a sealed flask, esterified compound (**E1-E3**), tris(hydroxymethyl)aminomethane and K_2CO_3 were suspended in dry DMSO (30 mL) and stirred at 35 ºC for 24 h under nitrogen atmosphere. The reaction mixture was then poured into ice-water mixture and stirred for 10 min. The separated solid was filtered, washed with excess of water and dried at 50 ºC for 1 day.

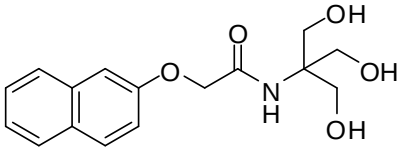

L1

*N-(1,3-dihydroxy-2-(hydroxymethyl)propan-2-yl)-2-(naphthalen-2-yloxy)acetamide, **L1***

The general procedure as above was followed using **E1** (3.0 g, 13.04 mmol), K_2CO_3 (3.6 g, 26.08 mmol) and tris(hydroxymethyl)aminomethane (1.89 g, 15.65 mmol) to get the ligand **L1**. Yield: 2.2 g (55.25%). Mp. 128-132 ºC. FT-IR: ν_{max}/cm^{-1} 3371 (ν OH), 3249 (ν NH), 1657 (ν C=O), 1535 (ν C=C), 1261-1218-1060 (ν C-O) cm^{-1}. ^{1}H NMR (500 MHz, DMSO-d_6): δ = 7.83 (m, 3H, ArH), 7.46 (t, 1H, J = 7.40 Hz, ArH), 7.36 (m, 2H, ArH), 7.29 (s, 1H, NH), 7.23 (dd, 1H, J = 2.25 & 8.57 Hz, ArH), 4.84 (t, 3H, J = 5.75 Hz, OH), 4.60 (s, 2H, OCH_2), 3.62 (d, 6H, J = 5.70 Hz, tris OCH_2). ^{13}C NMR (DMSO-d_6, 125 MHz): δ167.96, 155.30,

134.15, 129.56, 128.90, 127.62, 126.92, 126.63, 124.08, 118.51, 107.72, 67.25, 61.97, 60.05. ESI-MS: *m/z* [M+H] calcd. for $C_{16}H_{19}NO_5$: 306.1297; found: 306.1336.

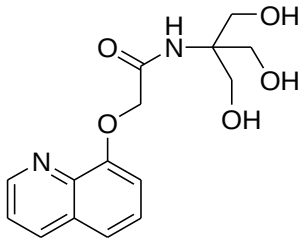

L2

N-(1,3-dihydroxy-2-(hydroxymethyl)propan-2-yl)-2-(quinolin-8-yloxy)acetamide, ***L2***

The general procedure as above was followed using **E2** (3.0 g, 12.97 mmol), K_2CO_3 (3.58 g, 25.94 mmol) and tris(hydroxymethyl)aminomethane (1.88 g, 15.56 mmol) to get the ligand **L2**. Yield: 2.60 g (65.44%). Mp.130-136 ºC. FT-IR: ν_{max}/cm^{-1} 3396 (ν OH), 3158 (ν NH), 1657 (ν C=O), 1529-1505-1426 (ν C=C), 1322, 1261-1108 (ν C-O) cm^{-1}. ^{1}H NMR (500 MHz, DMSO-d_6): δ = 8.88 (dd, 1H, *J* = 1.50 & 3.97 Hz, ArH), 8.34 (dd, 1H, *J* = 1.40 & 8.25 Hz, ArH), 7.76 (s, 1H, NH), 7.60-7.55 (m, 2H, ArH), 7.51 (t, 1H, *J* = 7.90 Hz, ArH), 7.28 (d, 1H, *J* = 7.50 Hz, ArH), 4.73 (t, 3H, *J* = 5.50 Hz, OH), 4.69 (s, 2H, OCH_2), 3.60 (d, 6H, *J* = 5.35 Hz, tris OCH_2). ^{13}C NMR (DMSO-d_6, 125 MHz): δ 168.42, 153.71, 149.45, 139.91, 135.95, 129.07, 126.76, 122.03, 121.20, 112.34, 69.30, 62.06, 60.01. ESI-MS: *m/z* [M+H] calcd. for $C_{15}H_{18}N_2O_5$: 307.1249; found: 307.1288.

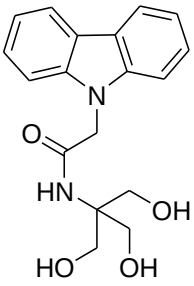

L3

2-(9H-carbazol-9-yl)-N-(1,3-dihydroxy-2-(hydroxymethyl)propan-2-yl)acetamide, ***L3***

The general procedure as above was followed using **E3** (3.0 g, 11.84 mmol), K_2CO_3 (3.2 g, 23.68 mmol) and tris(hydroxymethyl)aminomethane (1.72 g, 14.21 mmol) to get the ligand **L3**. Yield: 1.90 g (48.87%). Mp. 174-178 ºC. FT-IR: ν_{max}/cm^{-1} 3371(ν OH), 3292 (ν NH), 1645 (ν C=O), 1535-1462 (ν C=C), 1328, 1267-1212-1121 (ν C-O) cm^{-1}. ^{1}H NMR (500 MHz, DMSO-d_6): δ = 8.13 (d, 2H, *J* = 7.70 Hz, ArH), 7.62 (s, 1H, NH), 7.52 (d, 2H, *J* = 8.15 Hz, ArH), 7.41 (t, 2H, *J* = 7.45 Hz, ArH), 7.19 (t, 2H, *J* = 7.40 Hz, ArH), 5.06 (s, 2H, NCH_2), 4.67 (s, 3H, OH), 3.55 (s, 6H, tris OCH_2). ^{13}C NMR (DMSO-d_6, 125 MHz): δ 168.15, 140.60,

125.63, 122.13, 120.10, 118.93, 109.41, 62.47, 60.19, 45.72. ESI-MS (EI): *m/z* [M+H] calcd. for $C_{18}H_{20}N_2O_4$: 329.1457; found: 329.1496.

^{1}H NMR spectrum of **L1**

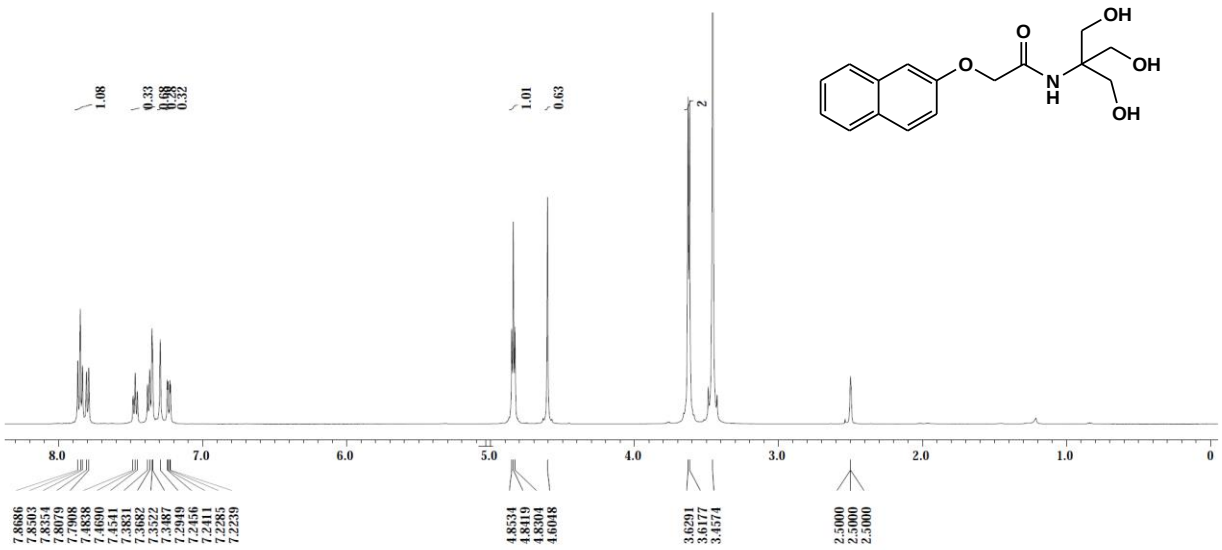

^{13}C NMR spectrum of **L1**

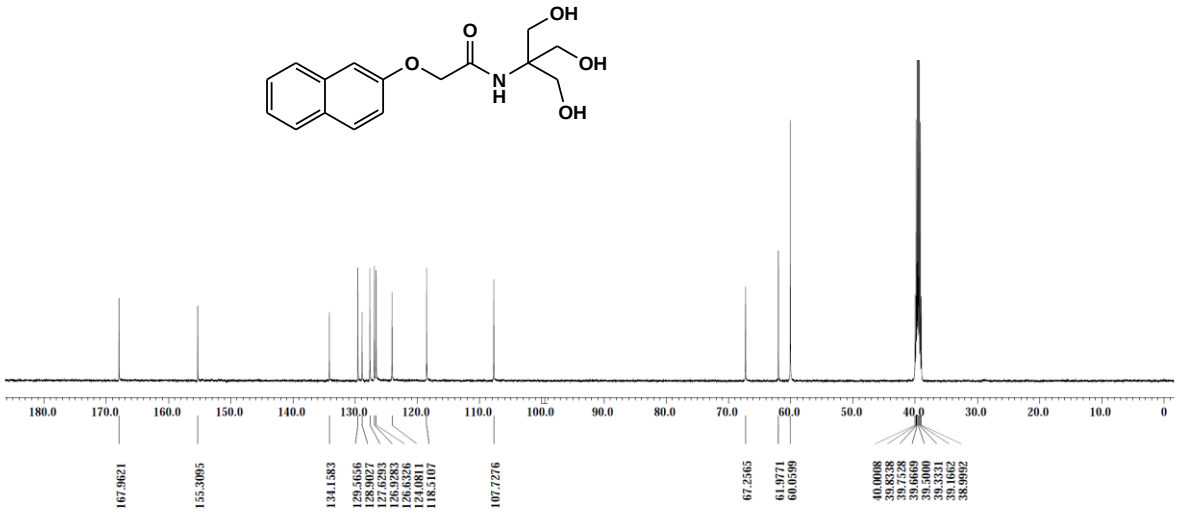

^{1}H NMR spectrum of **L2**

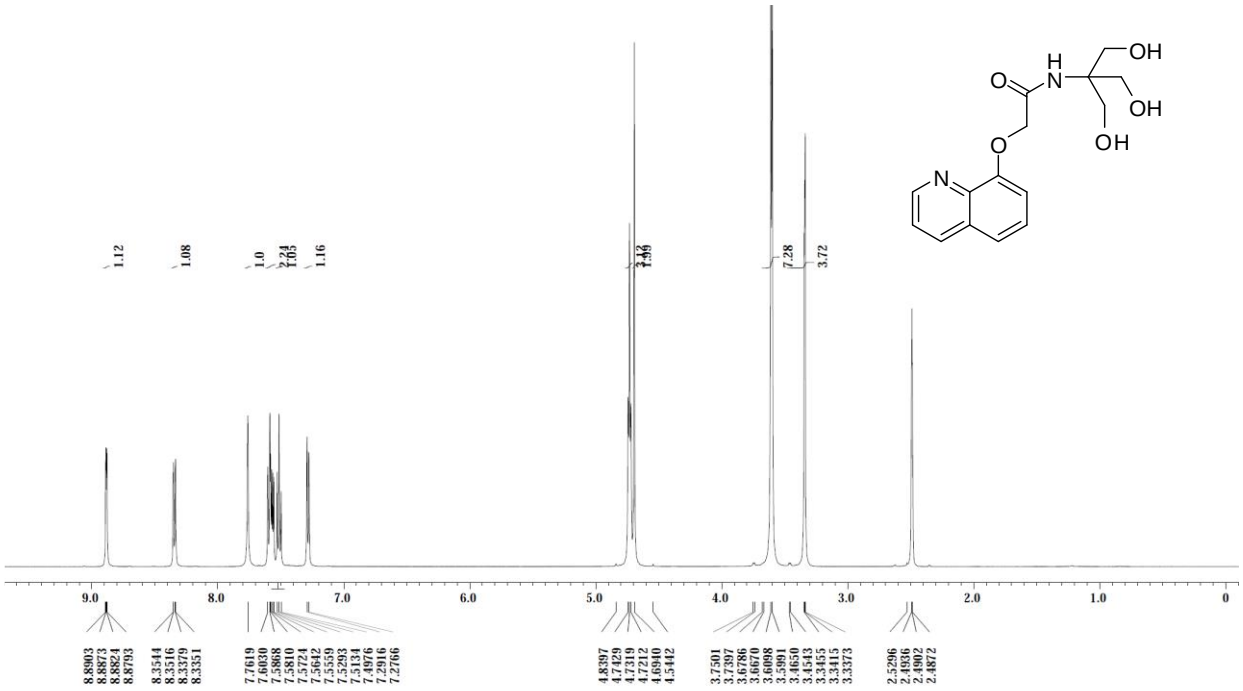

^{13}C NMR spectrum of **L2**

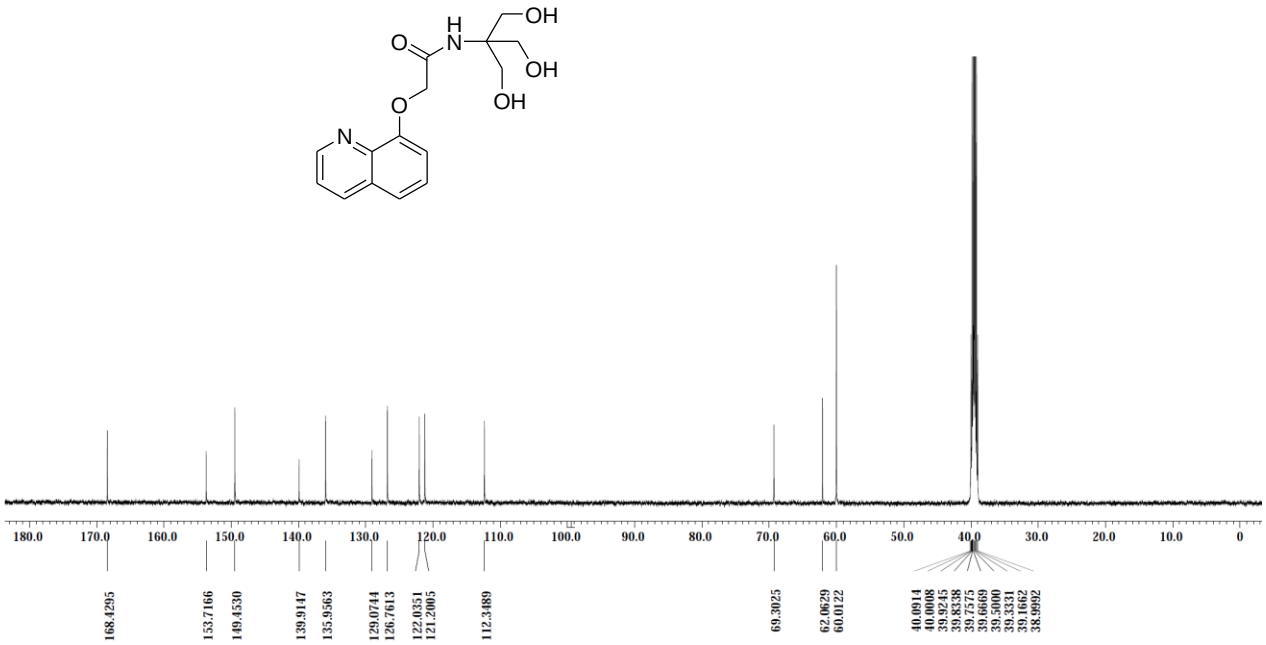

^{1}H NMR spectrum of **L3**

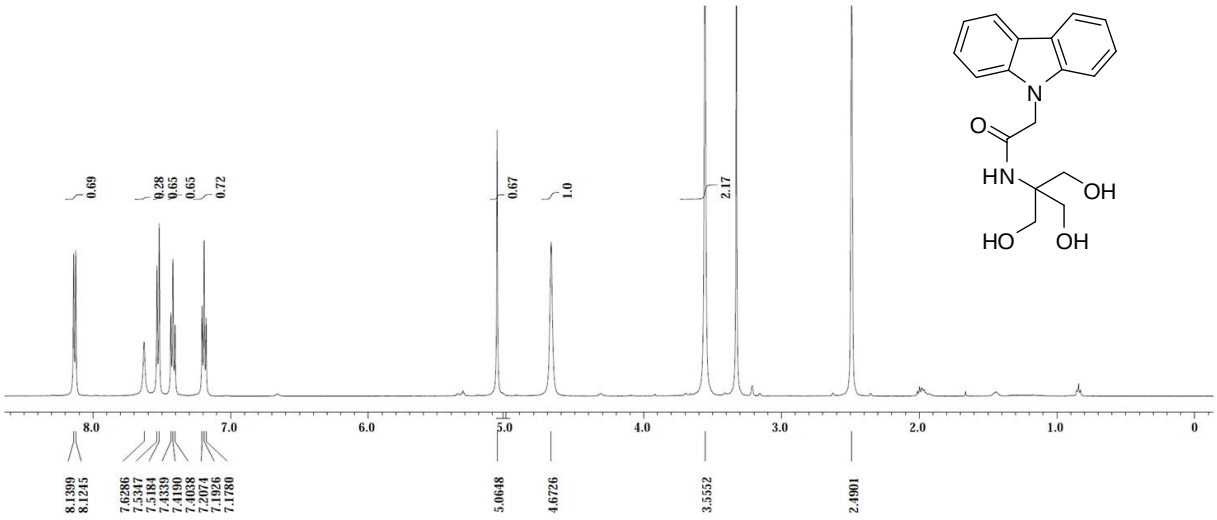

^{13}C NMR spectrum of **L3**

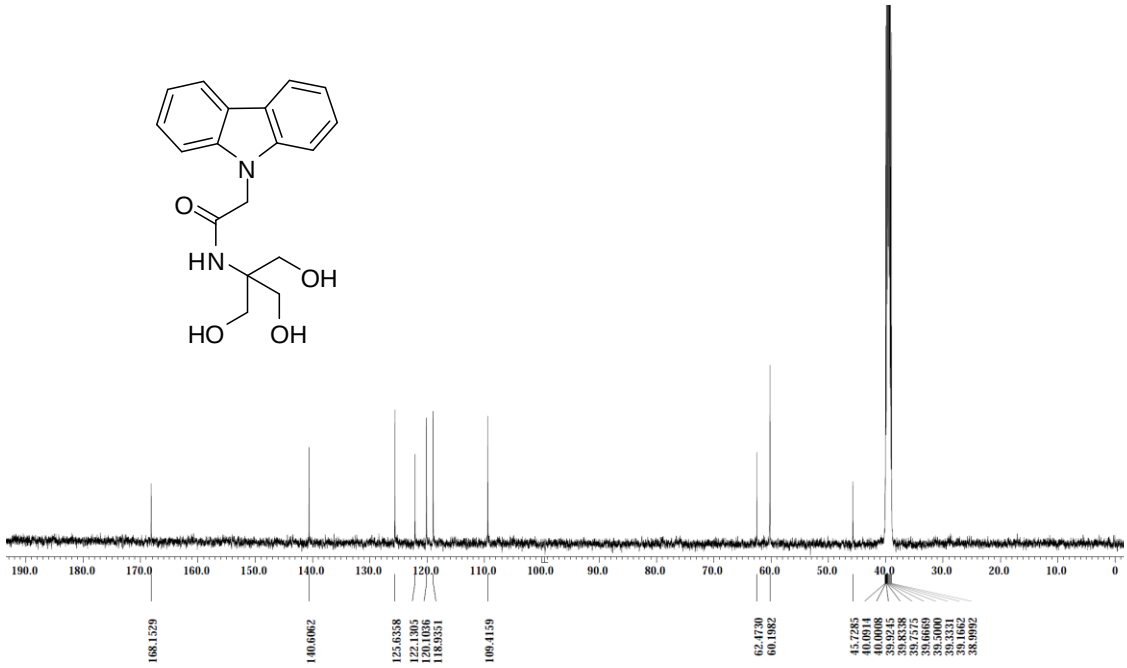

General procedure for the synthesis of hybrids M1-M3

$TBA_4[Mo_8O_{26}]$ (1 equiv.), $Mn(OAC)_3$ (1.5 equiv.) and **L1-L3** (3.5 equiv.) were introduced into a 100 mL round bottom flask under argon atmosphere. 20 mL of dry acetonitrile was added and the resulting mixture was refluxed under argon for 3 days. The reaction mixture was then cooled down to room temperature, filtered and added drop-wise into excess of diethyl ether under vigorous stirring. The resulting precipitate was collected, washed successively with 30 mL of ethanol and 30 mL of diethyl ether and then dried overnight in a desiccator. For growing single crystals, 100 mg of the product was dissolved in 15 mL of dry acetonitrile or dimethylformamide and the solution was evaporated slowly at room temperature. After three days, red colored crystals of the hybrids were collected from the solution.

Due to the presence of paramagnetic Mn(III) centers in **M1-M3,** their NMR spectra showed broad peaks.[10]

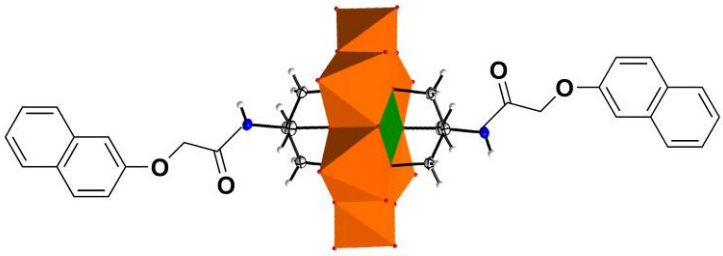

$TBA_3[MnMo_6O_{18}\{(OCH_2)_3C\text{-}NH\text{-}CO\text{-}C_{11}H_9O\}_2]$, ***M1***

The general procedure as above was followed using $TBA_4[Mo_8O_{26}]$ (0.3 g, 0.139 mmol), $Mn(OAC)_3$ (0.056 g, 0.209 mmol) and ligand **L1** (0.149 g, 0.487 mmol) to get the compound **M1**. Yield: 0.300 g (86.6 %). FT-IR: ν_{max}/cm^{-1} 2961-2872 (ν C−H), 1701 (ν C=O), 1628-1509-1481-1464 (ν C=C), 1385, 1215, 1119, 1063, 1029 (ν C−O), 921-938 (ν Mo=O), 667 (Mo−O−Mo) cm^{-1}. ^1H NMR (DMSO-d_6, 500 MHz): δ = 7.81-7.29 (m, br, 16H, ArH & NH), 4.90 (s, br, 4H, $ArOCH_2$), 3.13 (s, 24H, NCH_2), 1.53-1.29-0.91 (m, 84H, NCH_2CH_2, $NCH_2CH_2CH_2$, $NCH_2CH_2CH_2CH_3$), 64.66 (s, br, 12H, OCH_2). ^{13}C NMR (DMSO-d_6, 125 MHz): δ 168.80, 155.49, 133.73, 128.95, 128.31, 127.14, 126.49, 126.06, 123.35, 118.19, 106.98, 63.86, 57.19, 22.75, 19.01 and 13.31.

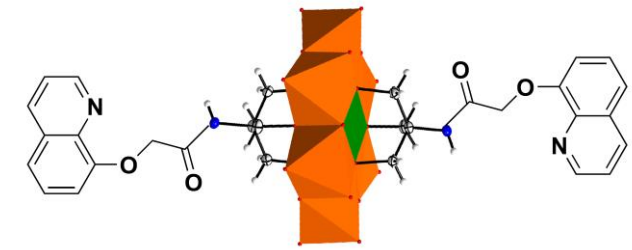

$TBA_3[MnMo_6O_{18}\{(OCH_2)_3C\text{-}NH\text{-}CO\text{-}C_{10}H_8NO\}_2]$, ***M2***

The general procedure as above was followed using $TBA_4[Mo_8O_{26}]$ (0.3 g, 0.139 mmol), $Mn(OAC)_3$ (0.056g, 0.209 mmol) and ligand **L2** (0.149 g, 0.487 mmol) to get the compound **M2**. Yield: 0.312 gm (89.96 %). FT-IR: ν_{max}/cm^{-1} 2961-2869 (ν C−H), 1684 (ν C=O), 1562-1482 (ν C=C), 1378, 1311, 1250, 1171, 1103, 1061, 1024 (ν C−O), 926 (ν Mo=O), 657 (ν Mo−O−Mo) cm^{-1}. ^{1}H NMR (DMSO-d_6, 500 MHz): δ = 8.84 (sbr, 4H, ArH), 8.35 (sbr, 2H, NH), 7.63-7.38 (mbr, 8H, ArH), 5.07 (sbr, 4H, $ArOCH_2$), 3.14 (s, 24H, NCH_2), 1.54-1.28-0.90 (m, 84H, NCH_2CH_2, $NCH_2CH_2CH_2$, $NCH_2CH_2CH_2CH_3$), 64.79 (sbr, 12H, OCH_2). ^{13}C NMR (DMSO-d_6, 125 MHz): δ 170.00, 154.26, 151.20, 140.01, 136.07, 128.84, 126.68, 121.91, 121.54, 114.40, 68.70, 57.24, 22.79, 19.07, 13.35.

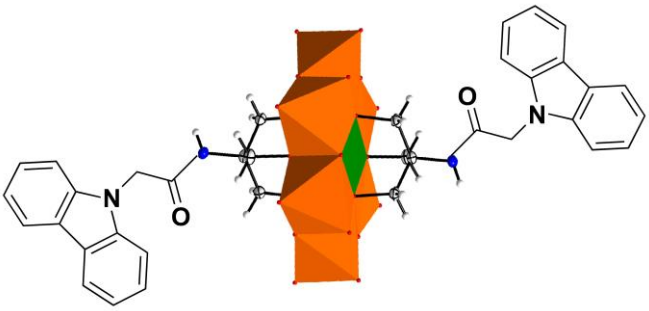

$TBA_3[MnMo_6O_{18}\{(OCH_2)_3C\text{-}NH\text{-}CO\text{-}C_{13}H_{10}N\}_2]$, ***M3***

The general procedure as above was followed using $TBA_4[Mo_8O_{26}]$ (0.3 g, 0.139 mmol), $Mn(OAC)_3$ (0.056 g, 0.209 mmol) and ligand **L3** (0.0160 g, 0.487 mmol) to get the compound **M3**. Yield: 0.340 gm (96.31%). FT-IR: ν_{max}/cm^{-1} 2963-2874 (ν C−H), 1696 (ν C=O), 1560-1460 (ν C=C), 1377, 1324, 1254, 1207, 1153, 1106, 1071, 1024 (ν C−O), 912 (ν Mo=O), 664 (Mo−O−Mo) cm^{-1}. ^{1}H NMR (DMSO-d_6, 500 MHz): δ = 8.13 (sbr, 4H, ArH), 7.47-7.20 (m, br, 14H, ArH & NH), 5.32 (sbr, 4H, $ArOCH_2$), 3.11 (s, 24H, NCH_2), 1.52-1.28-0.91 (m, 84H, NCH_2CH_2, $NCH_2CH_2CH_2$, $NCH_2CH_2CH_2CH_3$), 64.69 (sbr, 12H, OCH_2). ^{13}C NMR (DMSO-d_6, 125 MHz): δ 168.88, 140.42, 125.49, 121.84, 119.82, 118.60, 109.15, 60.33, 57.27, 42.16, 22.81, 19.04, 13.36.

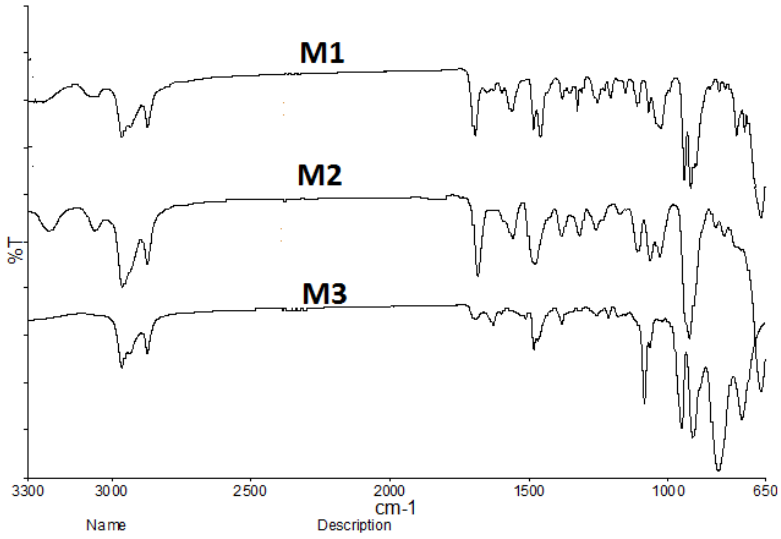

Figure S1. FT-IR spectra of hybrids **M1-M3**

^{1}H NMR spectrum of **M1**

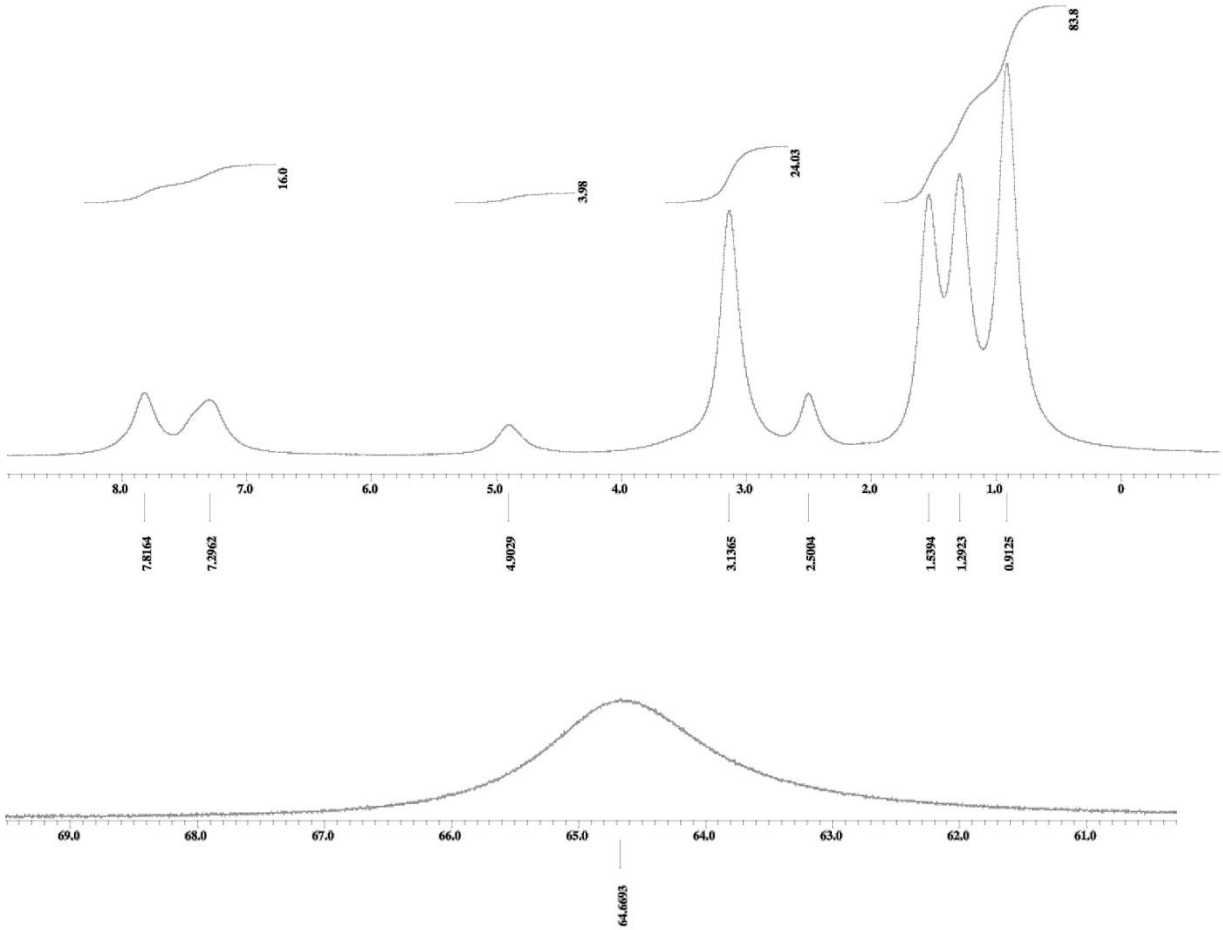

^{13}C NMR spectrum of **M1**

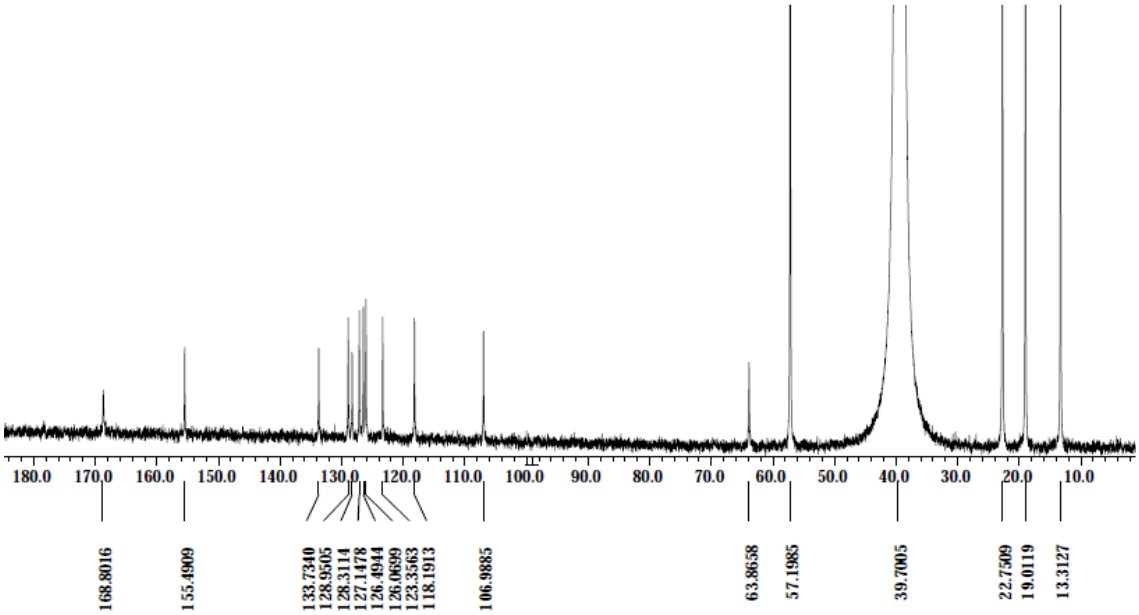

^{1}H NMR spectrum of **M2**

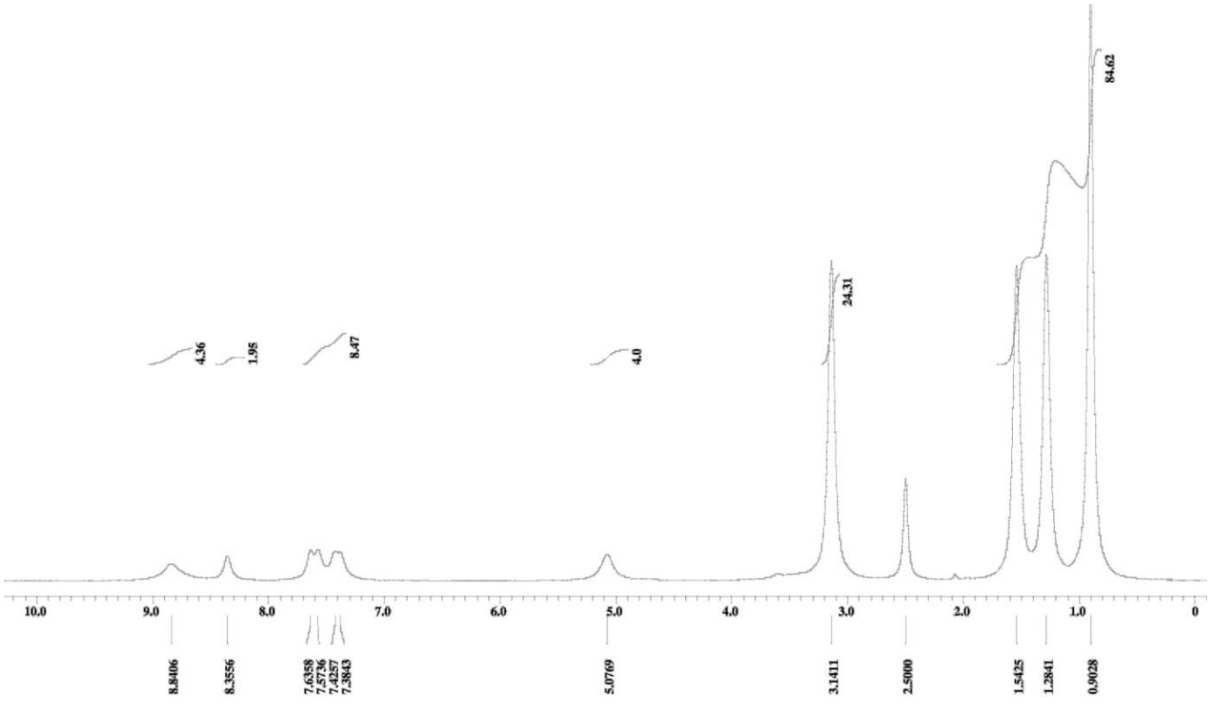

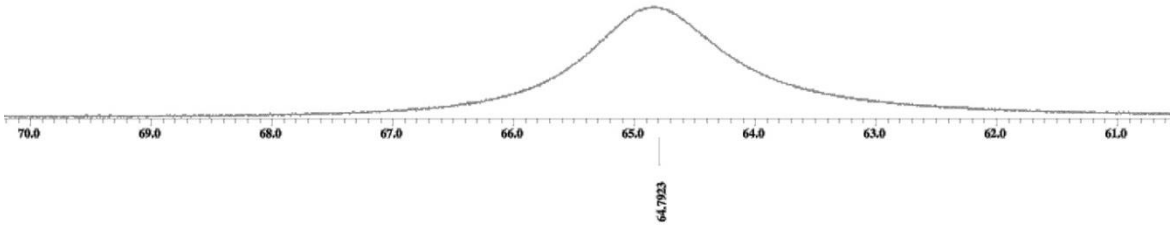

^{13}C NMR spectrum of **M2**

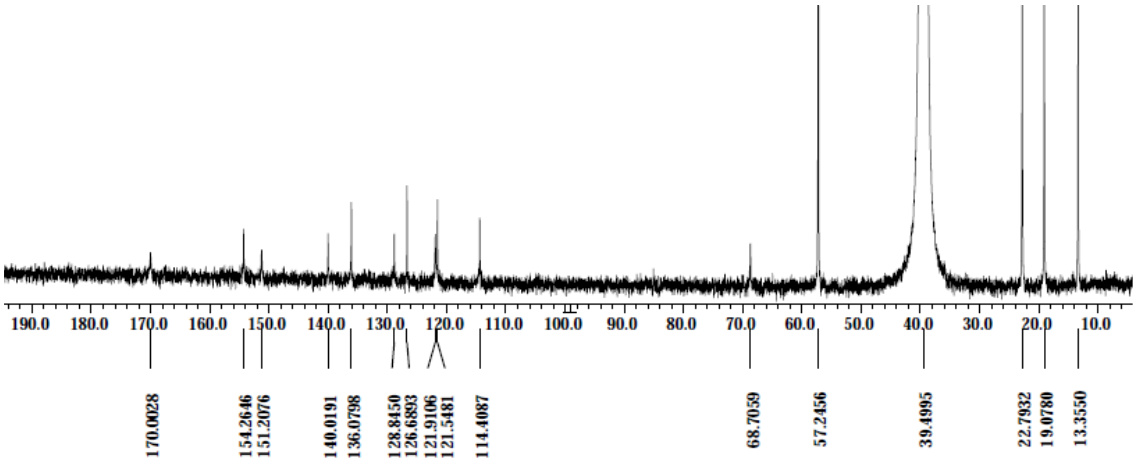

^{1}H NMR spectrum of **M3**

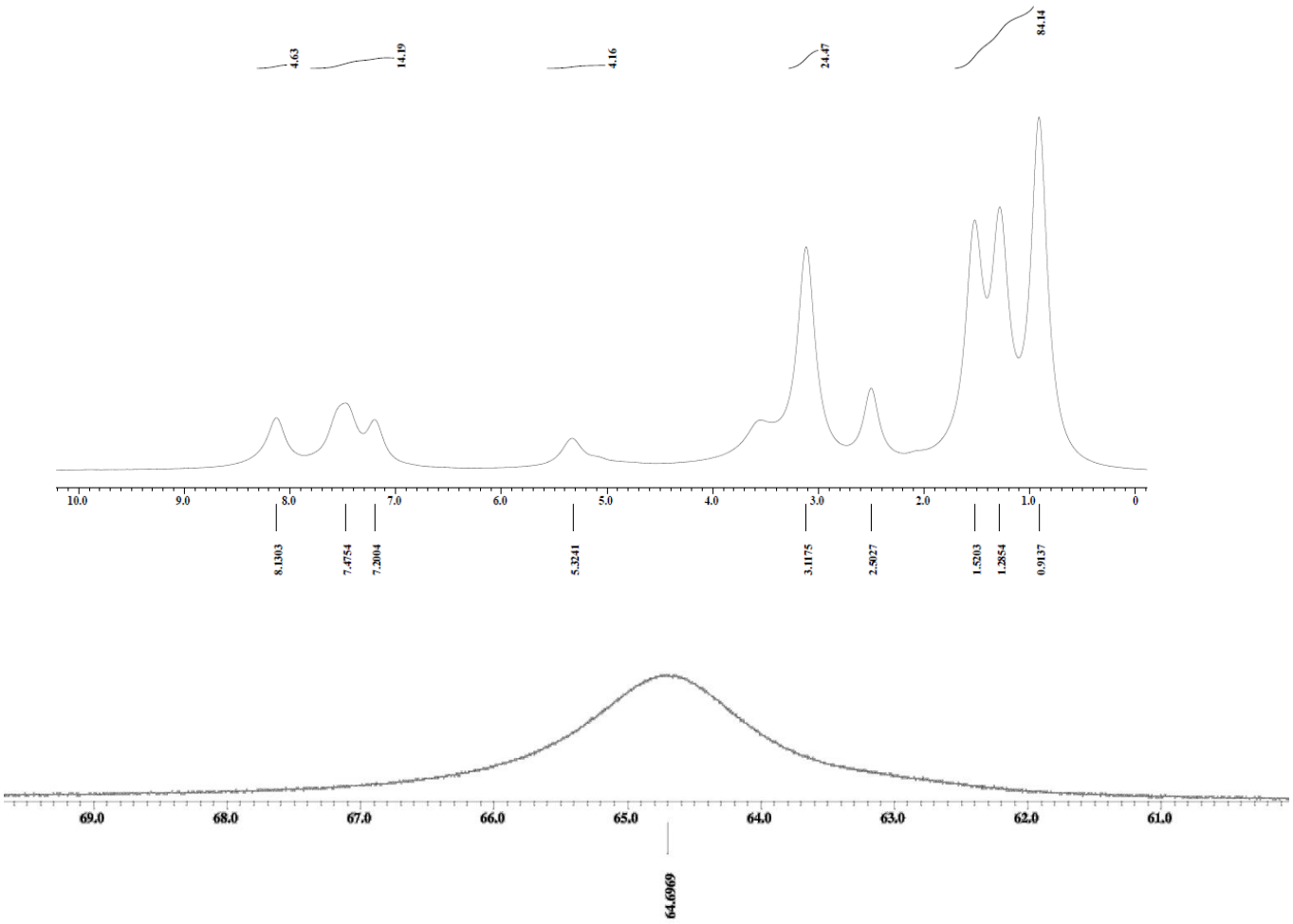

^{13}C NMR spectrum of **M3**

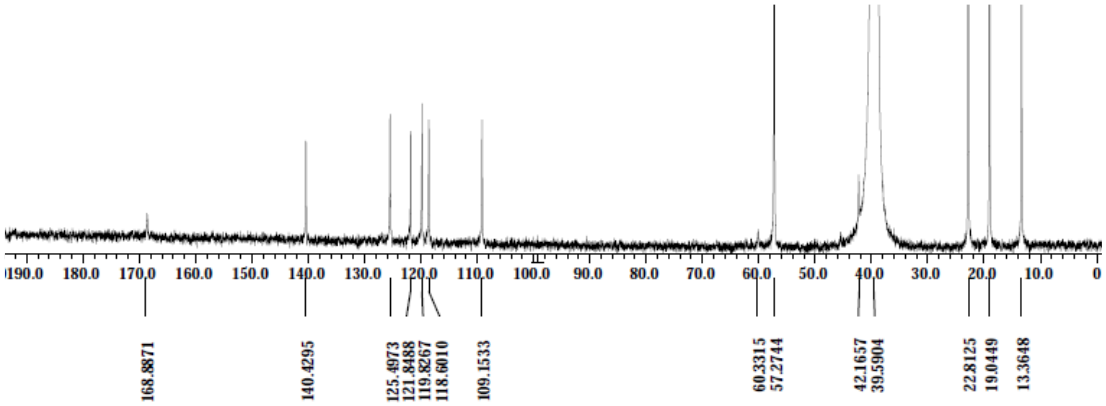

ESI-MS data of hybrids M1-M3

ESI-MS spectrum of **M1**

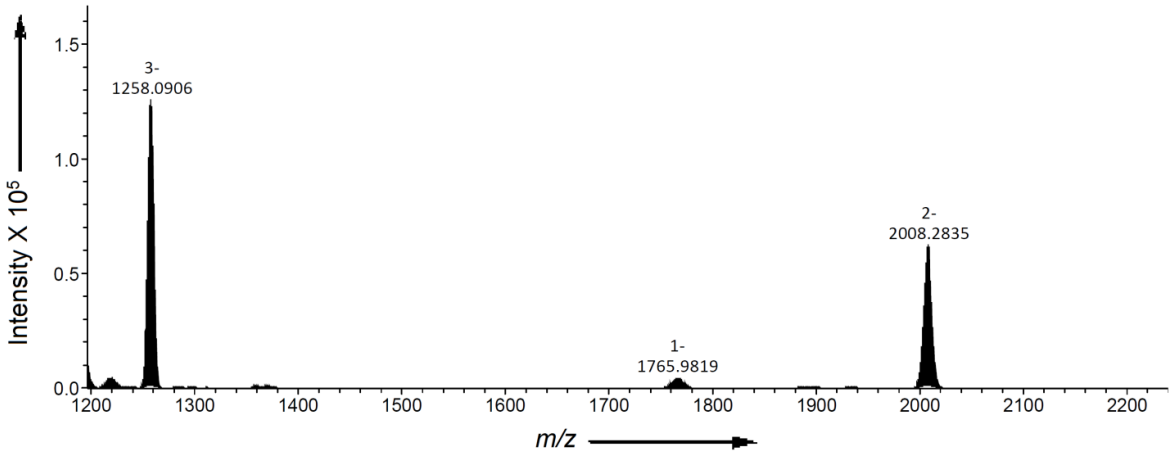

Figure S2. The negative ion mode ESI-MS spectrum of **M1** in acetonitrile

Table S1. Assignment of peaks in the mass spectrum of **M1**

S.No	Formula	Charge	m/z Calculated	m/z Observed
1	$TBA_3[MnMo_6O_{18}\{(OCH_2)_3C\text{-}NH\text{-}CO\text{-}C_{11}H_9O\}_2]_2$	-3	1257.91	1258.09
2	$(TBA)H[MnMo_6O_{18}\{(OCH_2)_3C\text{-}NH\text{-}CO\text{-}C_{11}H_9O\}_2]$	-1	1766.64	1765.98
3	$TBA_4[MnMo_6O_{18}\{(OCH_2)_3C\text{-}NH\text{-}CO\text{-}C_{11}H_9O\}_2]_2$	-2	2008.10	2008.28

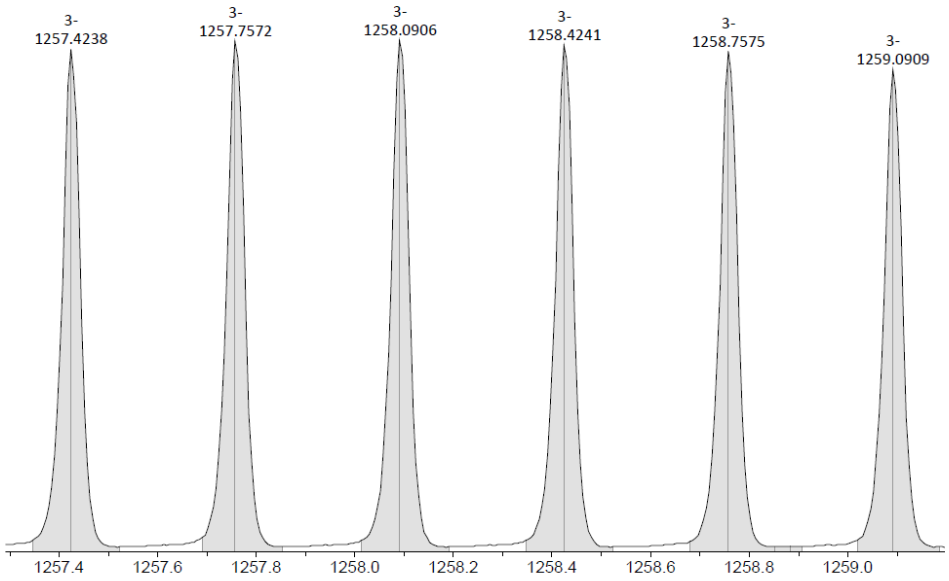

Figure S3. Zoom-in of the peak centered at around 1258.09 in the ESI-MS spectrum of **M1** to show the 3^- charge state

ESI-MS spectrum of **M2**

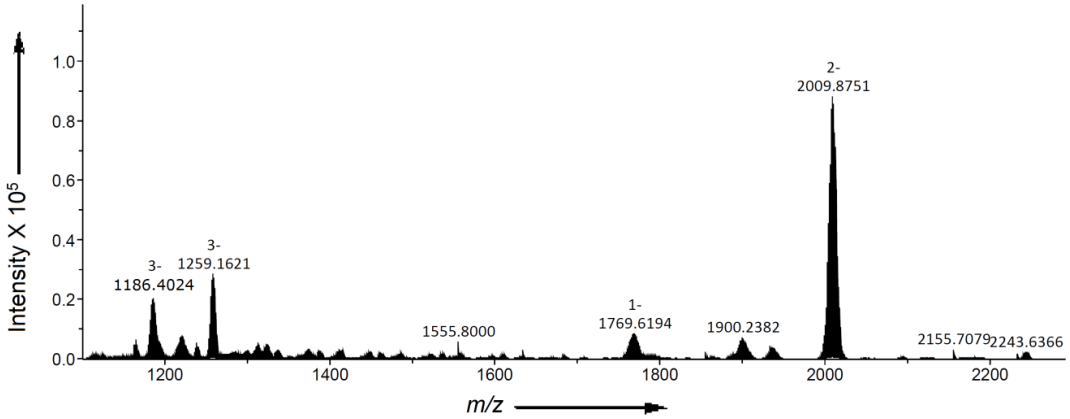

Figure S4. The negative ion mode ESI-MS spectrum of **M2** in acetonitrile

Table S2. Assignment of peaks in the mass spectrum of **M2**

S. No	Formula	Charge	m/z Calculated	m/z Observed
1	$(TBA)_2Na[MnMo_6O_{18}\{(OCH_2)_3C\text{-}NH\text{-}CO\text{-}C_{10}H_8NO\}_2]_2$	-3	1186.07	1186.40
2	$TBA_3[MnMo_6O_{18}\{(OCH_2)_3C\text{-}NH\text{-}CO\text{-}C_{10}H_8NO\}_2]_2$	-3	1259.23	1259.16
3	$(TBA)H[MnMo_6O_{18}\{(OCH_2)_3C\text{-}NH\text{-}CO\text{-}C_{10}H_8NO\}_2]$	-1	1768.62	1769.61
4	$TBA_4[MnMo_6O_{18}\{(OCH_2)_3C\text{-}NH\text{-}CO\text{-}C_{10}H_8NO\}_2]_2$	-2	2010.07	2009.87

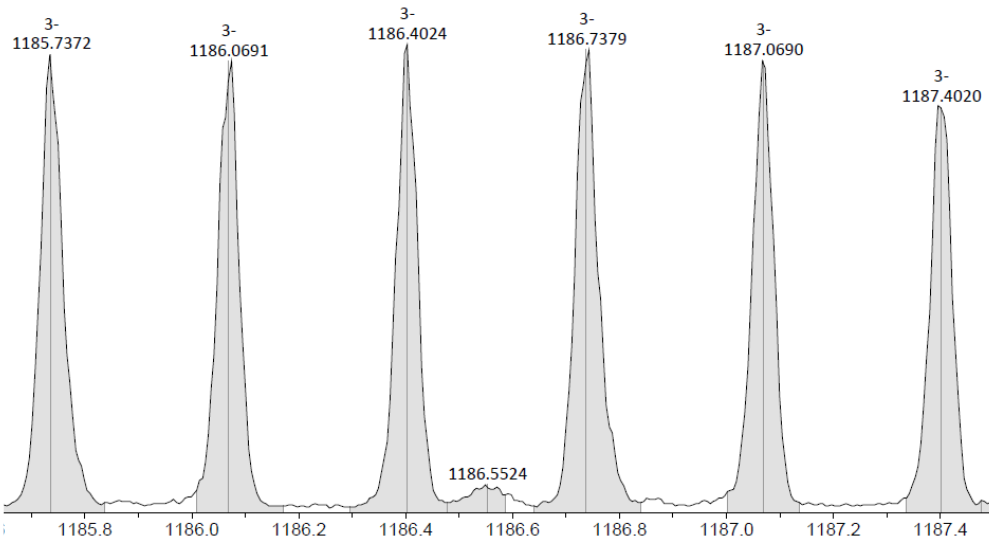

Figure S5. Zoom-in of the peak centered at around 1186.40 in the ESI-MS spectrum of **M2** to show the 3^- charge state

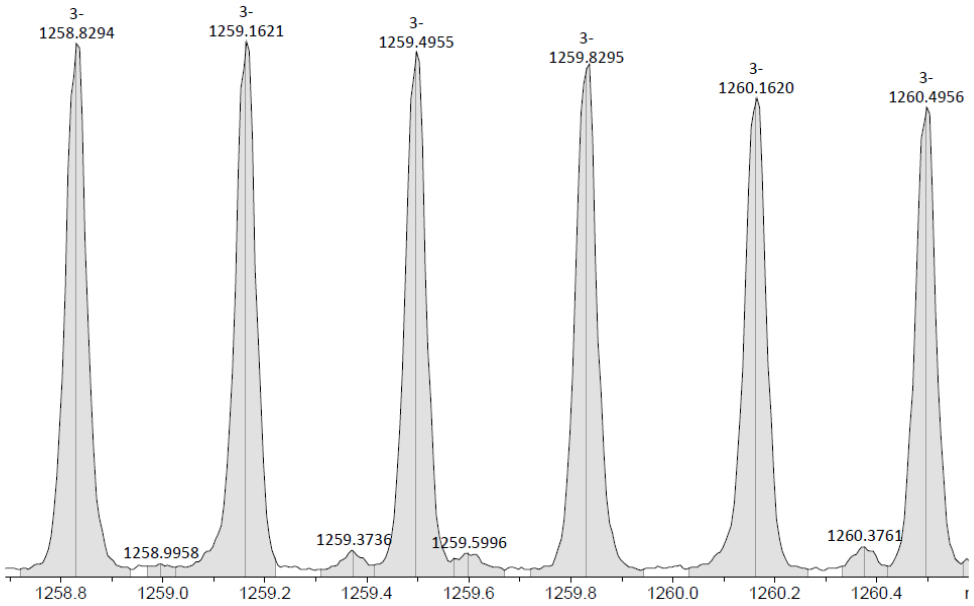

Figure S6. Zoom-in of the peak centered at around 1259.16 in the ESI-MS spectrum of **M2** to show the 3^- charge state

ESI-MS spectrum of **M3**

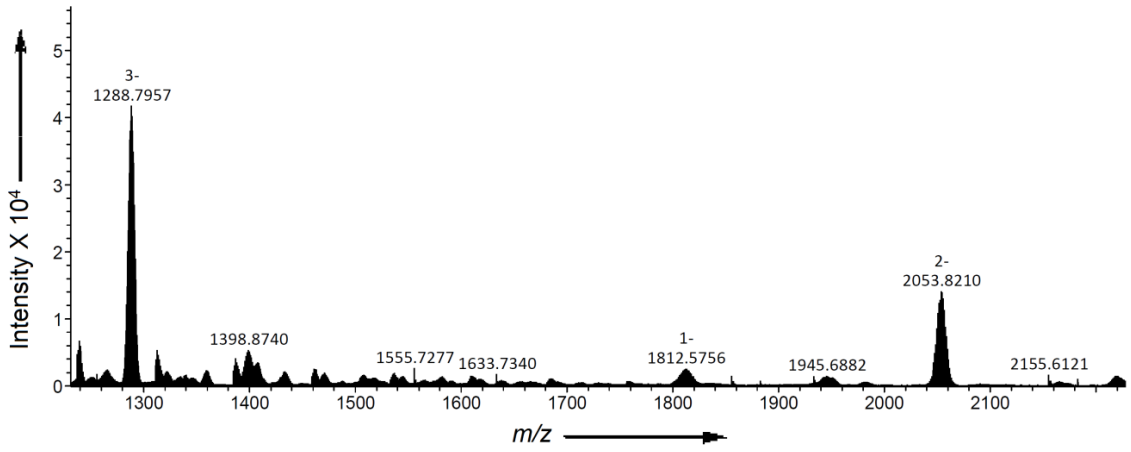

Figure S7. The negative ion mode ESI-MS spectrum of **M3** in acetonitrile

Table S3. Assignment of peaks in the mass spectrum of **M3**

S.No	Formula	Charge	m/z Calculated	m/z Observed
1	$TBA_3[MnMo_6O_{18}\{(OCH_2)_3C\text{-}NH\text{-}CO\text{-}C_{13}H_{10}N\}_2]_2$	-3	1288.62	1288.79
2	$(TBA)H[MnMo_6O_{18}\{(OCH_2)_3C\text{-}NH\text{-}CO\text{-}C_{13}H_{10}N\}_2]$	-1	1812.72	1812.57
3	$TBA_4[MnMo_6O_{18}\{(OCH_2)_3C\text{-}NH\text{-}CO\text{-}C_{13}H_{10}N\}_2]_2$	-2	2054.17	2053.82

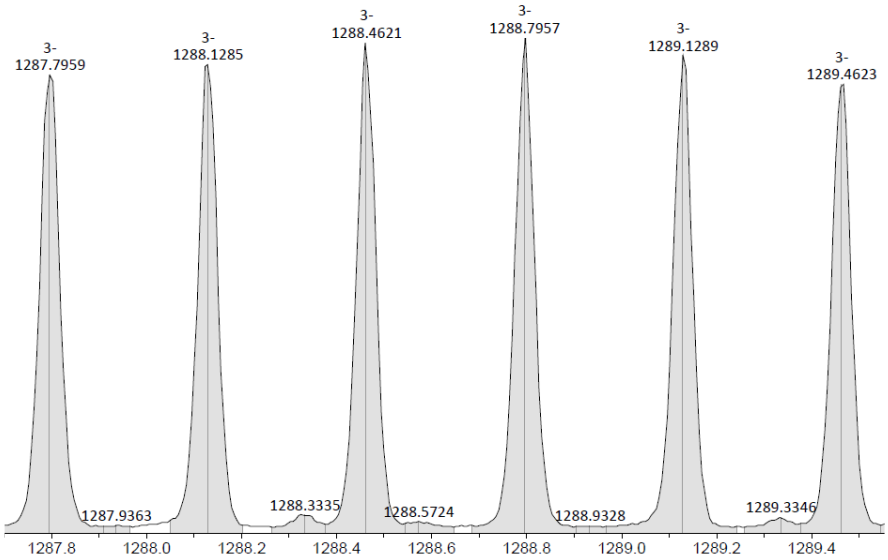

Figure S8. Zoom-in of the peak centered at around 1288.79 in the ESI-MS spectrum of **M3** to show the 3^- charge state

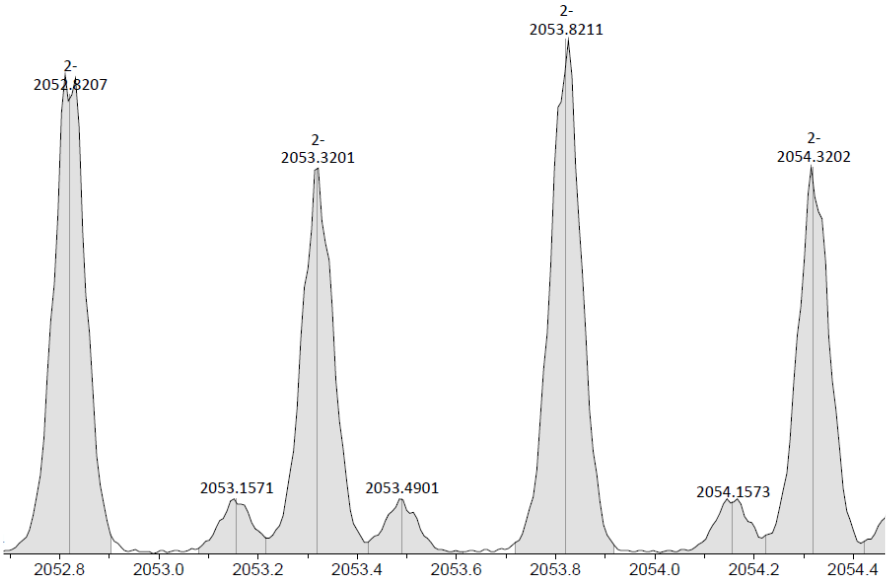

Figure S9. Zoom-in of the peak centered at around 2053.82 in the ESI-MS spectrum of **M3** to show the 2^- charge state

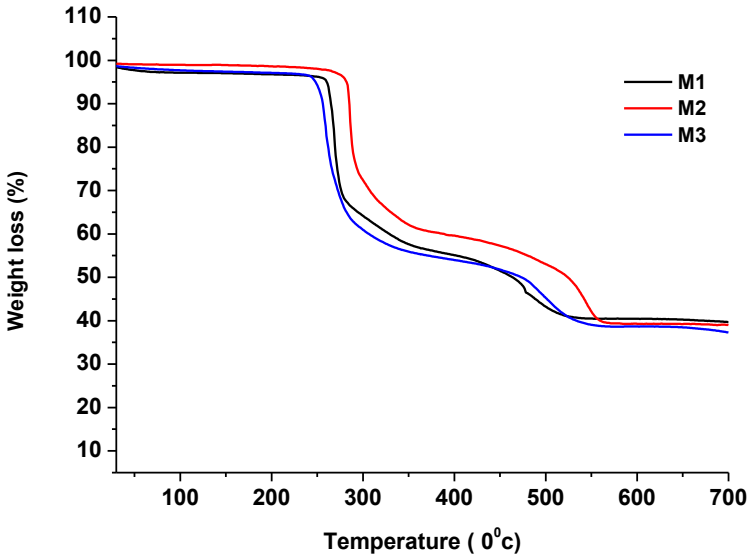

Figure S10. TGA plots of compounds **M1-M3** at a heating rate of 10 °C min^{-1} under N_2 atmosphere

Table S4. Crystal and structure refinement data for **M1** and **M2**

compounds	**M1**	**M2**
Empirical formula	$C_{90}H_{155}MnMo_6N_{10}O_{28}$	$C_{84}H_{152}MnMo_6N_9O_{30}$
Formula weight	2455.81	2398.72
Temperature	150(2) K	150(2) K
Wavelength	0.71073 Å	0.71073 Å
Crystal system	Monoclinic	Monoclinic
Space group	P 21/c	*P* 21/*c*
Unit cell dimensions	*a* = 26.4131(3) Å	*a* = 19.1909(3) Å
	b = 23.2246(2) Å *β*= 103.9230(10)°.	*b* = 19.5198(3) Å *β*= 97.562(2)°.
	c = 17.9467(2) Å	*c* = 27.7496(4) Å
Volume	10685.7(2) $Å^3$	10304.7(3) $Å^3$
Z	4	4
Density (calculated)	1.527 Mg/m^3	1.546 Mg/m^3
Absorption coefficient	0.871 mm^{-1}	0.902 mm^{-1}
F(000)	5064	4944
Crystal size	0.2883 x 0.2316x 0.2048 mm^3	0.1896 x 0.1670 x 0.1042 mm^3
Index ranges	-39<=h<=39, -33<=k<=33, -25<=l<=26	-25<=h<=25, -23<=k<=25, -35<=l<=36
Reflections collected	126647	111668
Independent reflections	35137 [R(int) = 0.0311]	23582 [R(int) = 0.0285]
Completeness to theta = 25.242°	99.8 %	100.0 %
Refinement method	Full-matrix least-squares on F^2	Full-matrix least-squares on F^2
Data / restraints / parameters	35137 / 0 / 1119	23582 / 0 / 1093
Goodness-of-fit on F^2	1.047	1.058
Final R indices [I>2sigma(I)]	R1 = 0.0401, wR2 = 0.0886	R1 = 0.0304, wR2 = 0.0739
R indices (all data)	R1 = 0.0565, wR2 = 0.0974	R1 = 0.0365, wR2 = 0.0767
Largest diff. peak and hole	3.326 and -1.058 $e.Å^{-3}$	1.114 and -0.927 $e.Å^{-3}$

Table S5. Details of the H-bonding interactions in **M1**

D-H...A	d(D-H)	d(H...A)	d(D...A)	<(DHA)
C(28)-H(28)...O(8)	0.95	2.58	3.518(3)	166.06
C(12)-H(12)...O(21)	0.95	2.55	3.437(3)	155.54
C(1)-H(1A)...O(13)#1	0.99	2.55	3.163(3)	119.8
C(2)-H(2B)...O(13)#1	0.99	2.46	3.059(3)	118.4
C(3)-H(3B)...N(10)#1	0.99	2.68	3.336(4)	124.0
C(17)-H(17A)...O(27)#2	0.99	2.27	2.896(3)	120.3
C(33)-H(33A)...O(27)	0.99	2.28	3.246(3)	166.3
C(33)-H(33B)...O(16)	0.99	2.48	3.461(3)	168.8
C(41)-H(41B)...O(4)	0.99	2.47	3.345(3)	146.5
C(38)-H(38B)...O(16)	0.99	2.49	3.429(4)	159.3
C(46)-H(46A)...O(2)	0.99	2.58	3.369(4)	136.7
C(46)-H(46B)...O(13)	0.99	2.60	3.529(4)	156.2
C(61)-H(61A)...O(18)#3	0.99	2.44	3.348(3)	152.3
C(50)-H(50B)...O(18)#3	0.99	2.53	3.481(4)	162.2
C(16)-H(16)...N(10)#1	0.95	2.66	3.488(4)	146.1
C(57)-H(57A)...O(16)	0.99	2.61	3.486(3)	147.2
C(70)-H(70B)...N(8)	0.99	2.65	3.459(6)	139.5
C(77)-H(77B)...O(5)#4	0.99	2.53	3.174(4)	122.3
C(73)-H(73A)...O(2)	0.99	2.55	3.156(4)	119.1
C(73)-H(73A)...O(9)#1	0.99	2.63	3.454(4)	141.1
C(74)-H(74A)...N(10)#4	0.99	2.65	3.511(5)	145.2
C(90)-H(90A)...O(3)	0.98	2.21	3.181(4)	168.6
C(86)-H(86A)...O(27)	0.98	2.51	3.321(5)	140.0
C(86)-H(86B)...O(19)	0.98	2.36	3.308(5)	162.7
C(82)-H(82B)...O(15)	0.98	2.45	3.305(6)	146.1
C(82)-H(82B)...O(18)	0.98	2.51	3.192(6)	126.9
C(82)-H(82C)...N(7)#5	0.98	2.60	3.468(10)	147.5
C(88)-H(88C)...O(8)	0.98	2.34	3.238(6)	151.8
C(84)-H(84B)...O(23)	0.98	2.49	3.386(6)	151.8
C(1)-H(1A)...O(13)#1	0.99	2.55	3.163(3)	119.8
C(2)-H(2B)...O(13)#1	0.99	2.46	3.059(3)	118.4

C(3)-H(3B)...N(10)#1	0.99	2.68	3.336(4)	124.0
C(17)-H(17A)...O(27)#2	0.99	2.27	2.896(3)	120.3
C(33)-H(33A)...O(27)	0.99	2.28	3.246(3)	166.3
C(33)-H(33B)...O(16)	0.99	2.48	3.461(3)	168.8
C(41)-H(41B)...O(4)	0.99	2.47	3.345(3)	146.5
C(38)-H(38B)...O(16)	0.99	2.49	3.429(4)	159.3
C(46)-H(46A)...O(2)	0.99	2.58	3.369(4)	136.7
C(46)-H(46B)...O(13)	0.99	2.60	3.529(4)	156.2
C(61)-H(61A)...O(18)#3	0.99	2.44	3.348(3)	152.3
C(50)-H(50B)...O(18)#3	0.99	2.53	3.481(4)	162.2
C(16)-H(16)...N(10)#1	0.95	2.66	3.488(4)	146.1
C(57)-H(57A)...O(16)	0.99	2.61	3.486(3)	147.2
C(70)-H(70B)...N(8)	0.99	2.65	3.459(6)	139.5
C(77)-H(77B)...O(5)#4	0.99	2.53	3.174(4)	122.3
C(73)-H(73A)...O(2)	0.99	2.55	3.156(4)	119.1
C(73)-H(73A)...O(9)#1	0.99	2.63	3.454(4)	141.1
C(74)-H(74A)...N(10)#4	0.99	2.65	3.511(5)	145.2
C(90)-H(90A)...O(3)	0.98	2.21	3.181(4)	168.6
C(86)-H(86A)...O(27)	0.98	2.51	3.321(5)	140.0
C(86)-H(86B)...O(19)	0.98	2.36	3.308(5)	162.7
C(82)-H(82B)...O(15)	0.98	2.45	3.305(6)	146.1
C(82)-H(82B)...O(18)	0.98	2.51	3.192(6)	126.9
C(82)-H(82C)...N(7)#5	0.98	2.60	3.468(10)	147.5
C(88)-H(88C)...O(8)	0.98	2.34	3.238(6)	151.8
C(84)-H(84B)...O(23)	0.98	2.49	3.386(6)	151.8

Symmetry transformations used to generate equivalent atoms:

#1 -x+1, -y+1, -z+3 #2 -x, -y+1, -z+2 #3 -x, y+1/2, -z+5/2

#4 -x+1, y-1/2, -z+5/2 #5 x, -y+1/2, z+1/2

Table S6. Details of the H-bonding interactions in **M2**

D-H...A	d(D-H)	d(H...A)	d(D...A)	<(DHA)
C(12)-H(12)...O(5)	0.93	2.30	3.176(5)	155.74
C(27)-H(27)...O(11) #3	0.93	2.55	3.272(4)	134.55
C(27)-H(27)...O(12) #3	0.93	2.41	3.263(4)	152.06
N(2)-H(2N)...N(4)	0.86	2.23	3.067(4)	163.3
N(1)-H(1N)...N(3)	0.86	2.31	3.163(4)	169.5
C(17)-H(17B)...O(27)	0.97	2.49	3.100(4)	120.4
C(4)-H(4A)...O(25)	0.97	2.38	2.985(4)	120.1
C(29)-H(29)...O(4)	0.93	2.59	3.455(5)	155.7
C(64)-H(64A)...O(25)#1	0.97	2.50	3.383(5)	150.9
C(71)-H(71B)...O(1)#1	0.97	2.47	3.380(5)	155.5
C(71)-H(71A)...O(25)#1	0.97	2.50	3.460(5)	171.4
C(67)-H(67B)...O(1)#1	0.97	2.59	3.471(5)	151.6
C(47)-H(47A)...O(8)#2	0.97	2.38	3.346(5)	173.9
C(75)-H(75A)...O(7)	0.97	2.50	3.190(5)	127.7
C(59)-H(59A)...O(11)#3	0.97	2.61	3.235(4)	122.1
C(63)-H(63A)...O(18)	0.97	2.36	3.199(4)	144.0
C(63)-H(63B)...O(7)	0.97	2.48	3.207(5)	132.0
C(56)-H(56A)...O(8)#2	0.97	2.55	3.139(5)	119.0
C(55)-H(55A)...O(12)#3	0.97	2.48	3.320(5)	145.3
C(55)-H(55B)...O(13)#3	0.97	2.44	3.182(4)	132.9
C(31)-H(31A)...N(4)#3	0.97	2.66	3.526(5)	148.5
C(31)-H(31B)...O(2)#3	0.97	2.54	3.511(5)	175.6
C(39)-H(39B)...O(5)	0.97	2.38	3.320(5)	163.5
C(40)-H(40B)...O(2)#3	0.97	2.64	3.379(5)	133.7
C(43)-H(43B)...O(6)	0.97	2.53	3.301(5)	136.6
C(72)-H(72B)...O(27)	0.97	2.40	3.364(5)	171.4

Symmetry transformations used to generate equivalent atoms:

#1 x,-y+3/2,z-1/2 #2 x-1,y,z #3 -x+1,y-1/2,-z+1/2

Self-assembly behavior of hybrids M1-M3 at different concentrations

10^{-3} M solutions of hybrids **M1-M3** in acetonitrile showed self-assembled structures of sizes **M1** = ~400 nm, **M2** = ~500 nm and **M3** = ~300 nm under TEM analyses. These results are in good agreement with the corresponding DLS data (**M1** = ~400-600 nm, **M2** = ~120-600 nm and **M3** = ~60-340 nm). To understand the effects of sample concentration in determining the self-assembly behaviors of hybrids **M1-M3** in solutions, DLS experiments were also conducted on 10^{-4} & 10^{-5} M solutions of **M1-M3** in acetonitrile. These studies revealed that the size of the self-assembled structures of **M1-M3** formed in solutions decreases with decrease in sample concentrations.[11] The DLS analysis results of hybrid compounds **M1-M3** are given in the Table S7.

Table S7. DLS data of hybrids **M1-M3** in different concentrations (10^{-3}, 10^{-4} and 10^{-5} M in acetonitrile).

Compounds	Concentration (ppm)	Particle size in DLS.
M1	10^{-3} M	400-600 nm
	10^{-4} M	105-190 nm
	10^{-5} M	37-68 nm
M2	10^{-3} M	120-600 nm
	10^{-4} M	91-141 nm
	10^{-5} M	32-43 nm
M3	10^{-3} M	60-340 nm
	10^{-4} M	50-78 nm
	10^{-5} M	8-15 nm

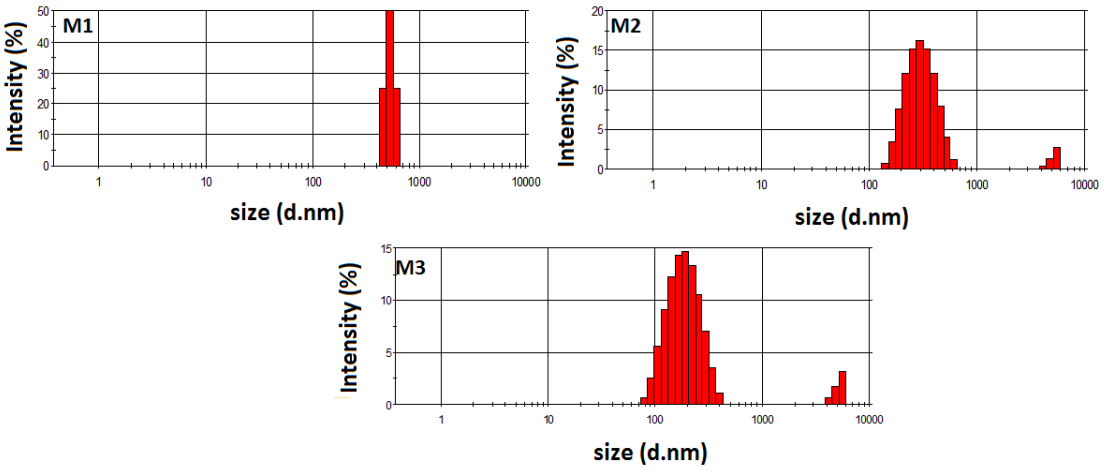

Figure S11. DLS plots of **M1-M3** hybrids in 10^{-3}M acetonitrile solutions

Self-assembly behaviors of hybrids M1-M3 in mixed MeCN-H_2O solvent system

The self-assembly properties of hybrids **M1-M3** in different MeCN-H_2O solvent systems were investigated and the results are tabulated in Table S8. It can be noted that on increasing the percentage of water (10-30%) in the solvent mixture, the size of the self-assembled structures increases. Probably this is due to the fact that the hybrids become less and less soluble on increasing the percentage of water in the solution, which tend to increase their aggregation behavior.[12] To confirm the shape and size of the self-assembled structures in MeCN-H_2O mixtures, TEM analyses were performed on one of the representative samples, i.e. solution of hybrid **M1** in MeCN-H_2O (30% of water) system. This study confirmed that **M1** forms large self-assembled structures of ~600 nm size in this mixed solvent system in agreement with the DLS results obtained (Figure S13 and Table S8).

Table S8. DLS data of **M1-M3** hybrids in 10^{-4} M MeCN-H_2O (water content 10-30%) solvent system.

Compounds	**% of water in 10^{-4} M ACN/H_2O system**	**Particle size in DLS.**
M1	10%	140-190 nm
	20%	122-615nm
	30%	105-825nm
M2	10%	220-326 nm
	20%	255-341 nm
	30%	295-458 nm
M3	10%	58-91 nm
	20%	68-105 nm
	30%	91-122 nm

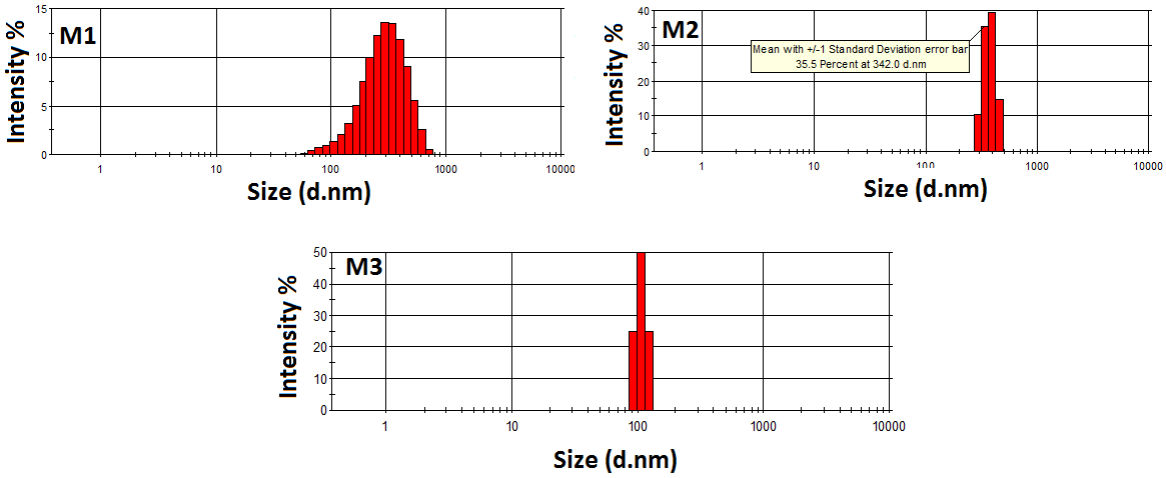

Figure S12. DLS graphs of **M1-M3** hybrids in 10^{-4} M MeCN-H_2O (water content 30%) solvent system

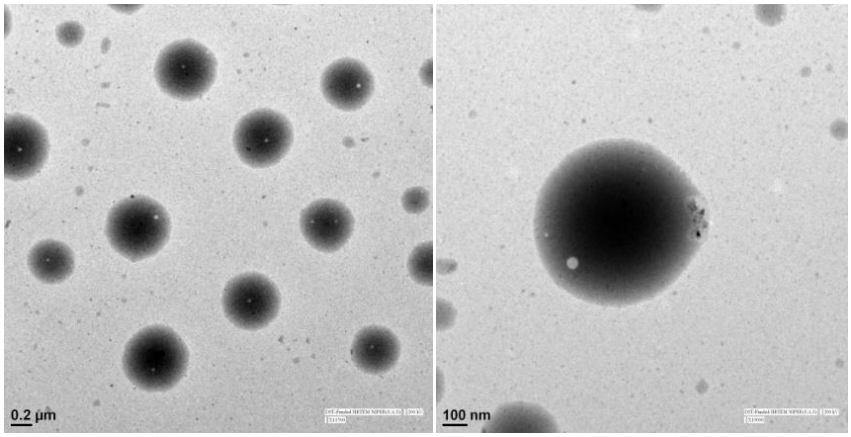

Figure S13. TEM images of the hybrid **M1** in ACN-H_2O system (water content 30%)

Self-assembly behaviors of hybrids M1-M3 in presence of an added salt $TBAPF_6$

Self-assembly properties of hybrids **M1-M3** in presence of an added salt like $TBAPF_6$ were studied and the results are presented in Table S9. 3 ml 10^{-3} M solutions of hybrids **M1-M3** in acetonitrile were selected for this study. The sequential addition of 5, 10, 15 and 20 mg of $TBAPF_6$ to this solution showed a decrease in the size of the self-assembled structures.[11]

TEM analyses were performed on a representative sample i.e. 3 ml solution of **M2** in MeCN in presence of low (15 mg) and high (50 mg) concentrations of $TBAPF_6$ to confirm the shape and size of the self-assembled structures. This study confirmed that the self-assembled structures formed are of size 350 nm in presence of 15 mg of $TBAPF_6$ and at higher concentrations of $TBAPF_6$ (50 mg), no self-assembled structures were observed, see Table S9 and Figures S14 and S15 for details.

These results are in agreement with the results of similar studies reported on Dawson cluster based hybrids in presence of added salts like tetrabutylammonium iodide (TBA.I) and dodecyltrimethylammonium bromide (DTMA·Br), where the self-assembled structures are found to disintegrate in highly ionic media.

Table S9. DLS data of 10^{-3} M solution of hybrids **M1-M3** in MeCN in presence of different amounts (5 to 50 mg) of an added salt $TBAPF_6$

Compounds	**Amount of $TBAPF_6$ in 10^{-3} M ACN solution**	**Particle size in DLS**
M1	5 mg	320-470 nm
	15 mg	190-250nm
	30 mg	43-91nm
	50 mg	8-28 nm
M2	5 mg	230-520 nm
	15 mg	320-400nm
	30 mg	68-105 nm
	50 mg	6-11 nm
M3	5 mg	130-220nm
	10 mg	90-150 nm
	30 mg	21-43 nm
	50 mg	1-4nm

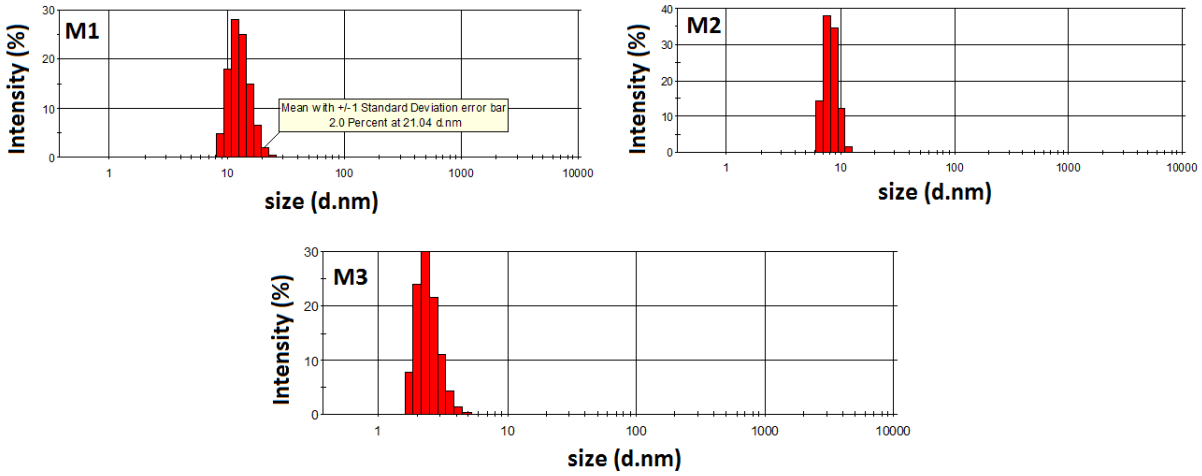

Figure S14. DLS plots of hybrids **M1-M3** in 10^{-3}**M** MeCN solution (3 ml) in presence of 50 mg of $TBAPF_6$

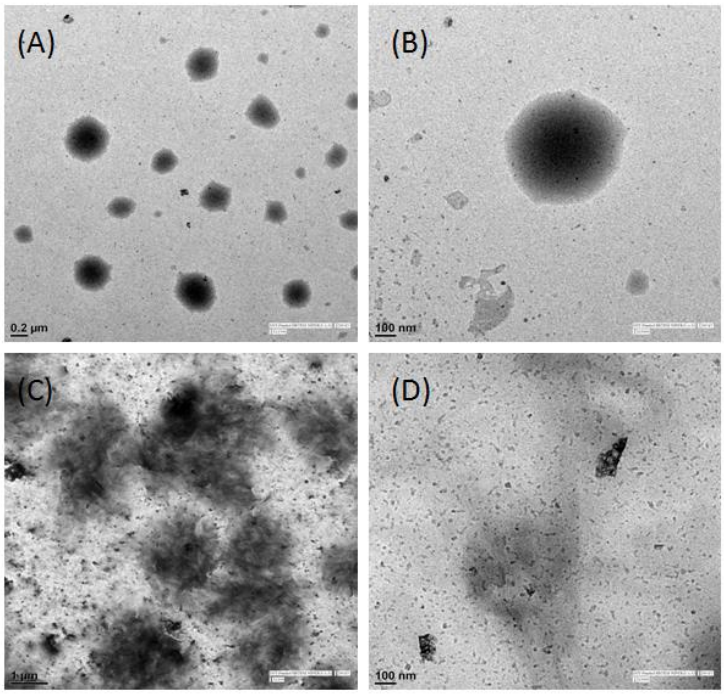

Figure S15. TEM images of hybrid **M2** in presence of 15 mg (images A and B) and 50 mg (images C and D) of $TBAPF_6$ in 10^{-3} M MeCN solution (3 ml)

Self-assembly behaviors of hybrids M1-M3 in mixed DMSO-H_2O solvent system

Finally, the self-assembly behaviors of hybrids **M1-M3** in DMSO-H_2O system were also studied. Solutions of hybrids **M1-M3** at 250 ppm concentration level in DMSO-H_2O mixed solvent system (which was used for the genotoxic studies) were selected for this study. TEM analysis on these solutions revealed the formation of spherical assemblies of the hybrids with sizes: **M1**, ~50 nm; **M2**, ~80 nm and **M3**, ~130 nm as shown in Fig. S16, which are in good agreement with the DLS results (**M1**, ~ 58-78 nm; **M2**, ~70-110 nm and **M3**, ~ 141-220 nm) as well, see Figures S16 and S17.

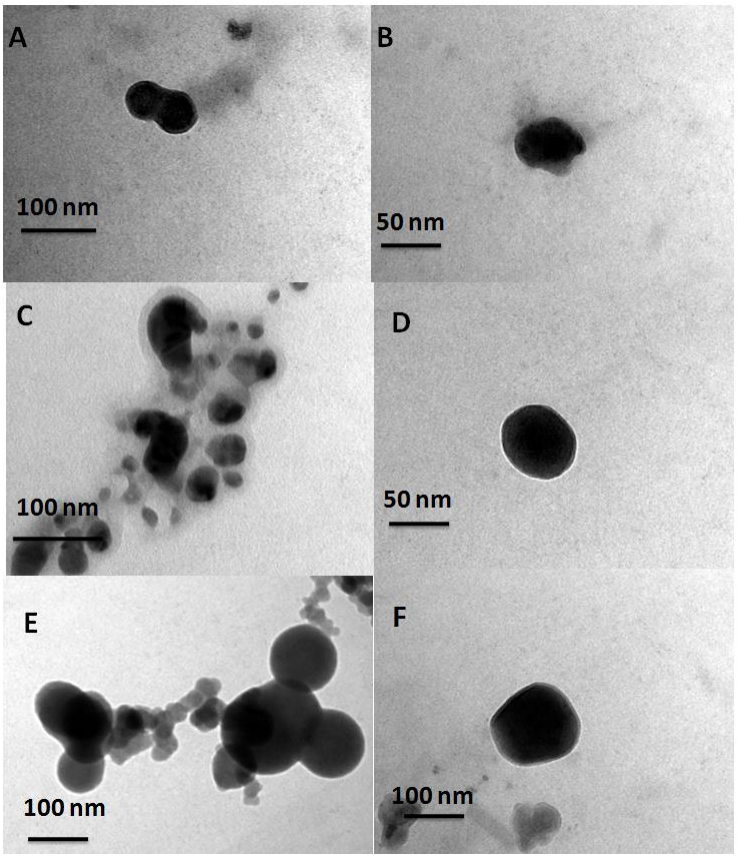

Figure S16. TEM images of the hybrids **M1** (A-B), **M2** (C-D) and **M3** (E-F) at 250 ppm concentration in mixed DMSO-H_2O solvent system

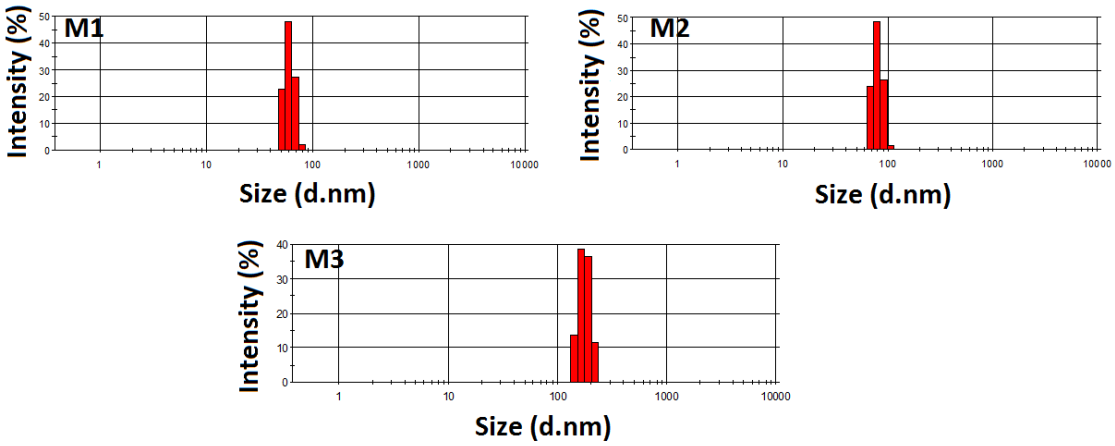

Figure S17. DLS plots of the hybrids **M1-M3** at 250 ppm concentration level in DMSO-H_2O mixed solvent system

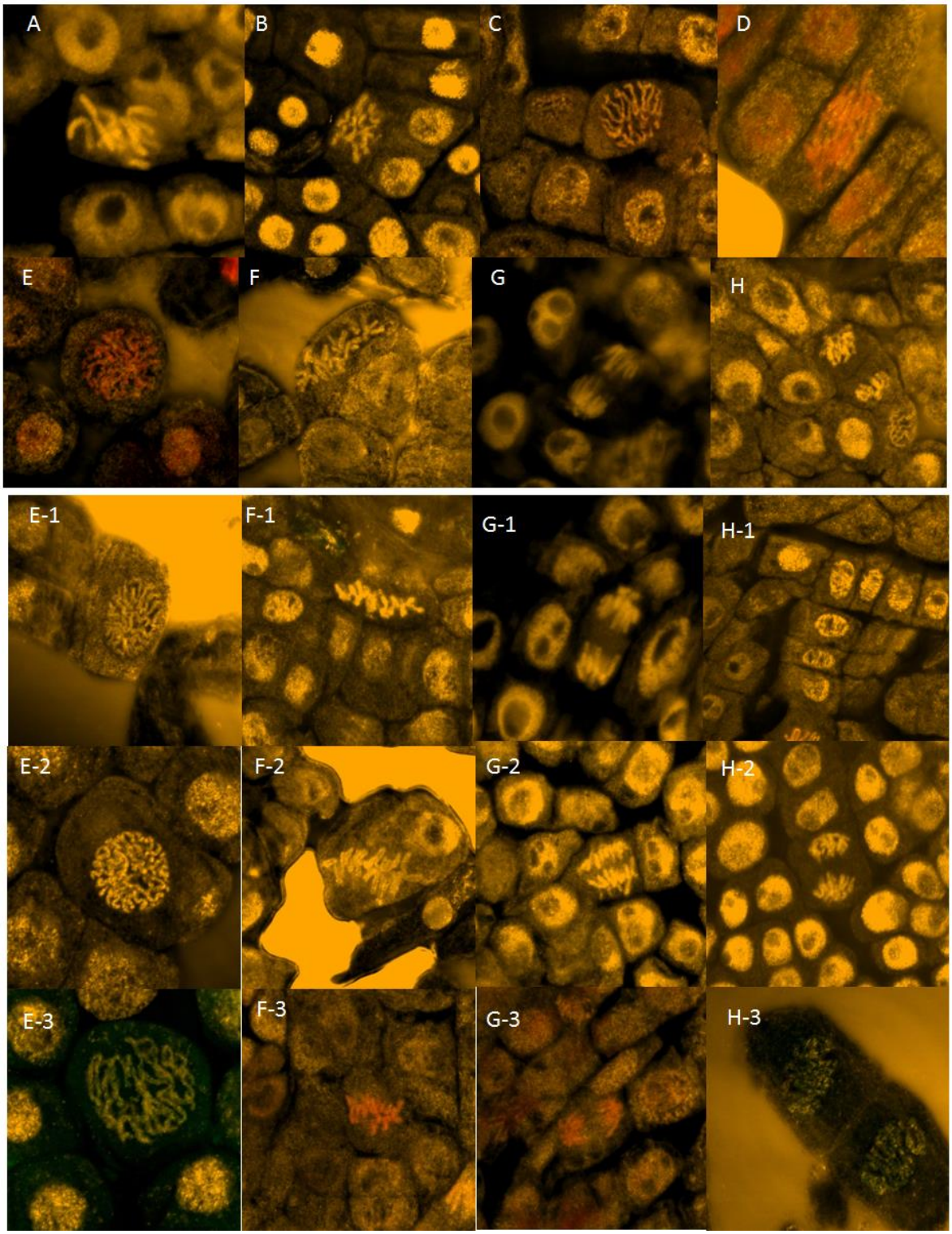
A
B
C
D
E
F
G
H
E-1
F-1
G-1
H-1
E-2
F-2
G-2
H-2
E-3
F-3
G-3
H-3

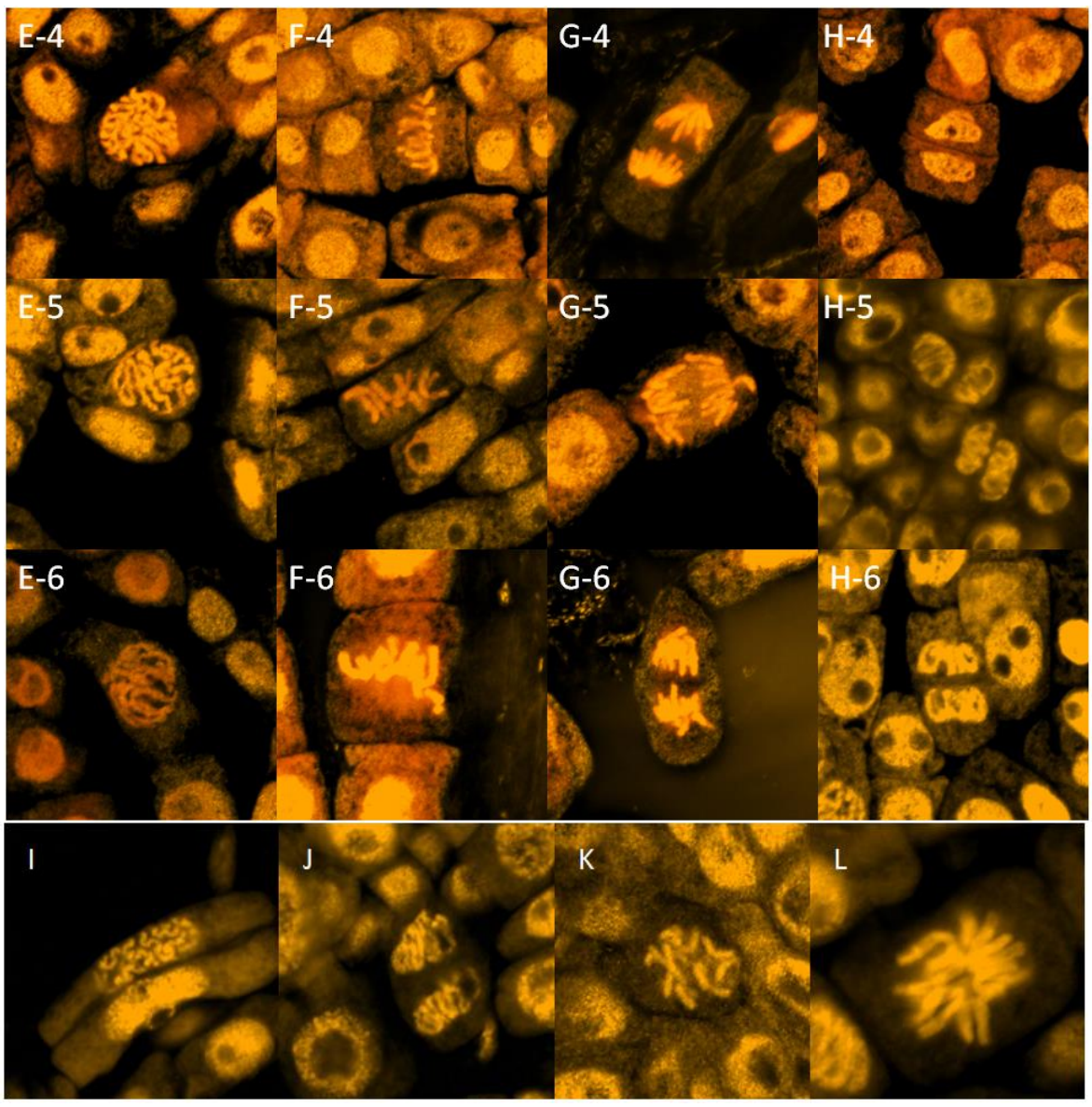

Figure S18. Cytotoxic damages observed in meristematic cells of *Allium cepa* roots treated with the H_2O_2 (positive control) (A-D), distilled water – DMSO mixture (negative control) (E-H), **M1** (E-1 to H-1), **M2** (E-2 to H-2), **M3** (E-3 to H-3), **L1** (E-4 to H-4), **L2** (E-5 to H-5), **L3** (E-6 to H-6) and **C1** (I-L). (A) sticky metaphase, (B) chromosomes breaks at anaphase, (C) irregular prophase, (D) anaphase bridge, (E) prophase, (F) metaphase, (G) anaphase, (H) telophase, (E-1) prophase, (F-1) metaphase, (G-1) anaphase, (H-1) telophase, (E-2) prophase, (F-2) metaphase, (G-2) anaphase, (H-2) telophase, (E-3) prophase, (F-3) metaphase, (G-3) anaphase, (H-3) telophase, (E-4) prophase, (F-4) metaphase, (G-4) anaphase, (H-4) telophase, (E-5) prophase, (F-5) metaphase, (G-5) anaphase, (H-5) telophase, (E-6) prophase, (F-6) metaphase, (G-6) anaphase, (H-6) telophase, (I) distributed pole to pole arrangement of chromosomes at metaphase, (J) telophase laggard, (K) vagrant chromosome and (L) stellate anaphase.

Table S10. Mitotic indices and chromosomal aberration indices observed in *Allium cepa* meristematic root tip cells exposed for 4 hours to different concentrations **L1-L3**

Treatment	Concentration (ppm)	No. of dividing cells	Mitotic Index MI (%)	No. of damaged cells	Chromosomal Aberration index CA (%)
L1	50	209	13.93±3.51	9	0.60±1.52
	150	192	12.80±3.05	10	0.66±1.0
	250	188	12.53±2.64	12	0.80±1.15
L2	50	213	14.20±4.04	11	0.73±1.52
	150	198	13.20±1.52	11	0.73±0.57
	250	192	12.80±3.05	13	0.86±2.0
L3	50	198	13.20±4.0	11	0.73±0.57
	150	187	12.46±3.21	13	0.86±1.15
	250	181	12.06±2.30	15	1.0±1.73

Mitotic and aberration indices were calculated as: (number of dividing cells or damaged cells/total number of cells observed) × 100.

The genotoxic properties of the organic moieties **L1**, **L2** and **L3** were also investigated as controls and the results are given in Table S10. The mitotic indices shown by **L1**, **L2** and **L3** at 250 ppm concentration were 12.53 %, 12.80 % and 12.06 % respectively; whereas the chromosomal aberration indices shown by **L1**, **L2** and **L3** at 250 ppm were 0.80 %, 0.86 % and 1.0 % respectively. These values are close to the mitotic and chromosomal aberrations exhibited by the negative control (distilled water-DMSO mixture) at 250 ppm level and thus show the relatively low toxic nature of these organic derivatives.

Genotoxicity tests using *Allium cepa* cells

The genotoxicity test was conducted according to a reported protocol[13] with slight modifications. Clean and healthy bulbs of *A. cepa* were selected for the study. The outer scales and dried roots were removed carefully without damaging the meristematic tissues. A series of six onion bulbs were placed in fresh distilled water for 72 h in dark. Distilled water was changed daily. After a period of 3 days, bulbs with best root growth (2–2.5 cm) were selected for the treatment. The standard 50, 150, 250 ppm solutions of $TBA_3[MnMo_6O_{18}\{(OCH_2)_3C\text{-}NH_2\}_2]$), **L1-L3** and **M1-M3** were prepared in DMSO which were then diluted with distilled water before the analyses. The roots separated from the bulb were exposed to different concentrations (50, 150 and 250 ppm) of the above solutions for a period of 4 h. As positive and negative controls, some root cells were treated with 250 ppm of H_2O_2 in distilled water (5mL) and different concentrations of distilled water-DMSO mixtures (5 mL) respectively. All the experiments were

carried out in triplicate. The chromosomal aberration was analysed by root meristem squash technique[14] using Nikon Eclipse LV100 POL optical microscopy. The root tips exposed to different concentrations of hybrids **M1-M3** were fixed in 95% ethanol and glacial acetic acid (3:1, v/v) for 5 minutes. After that, the solution was drained off and washed the root tips with distilled water. These were then macerated in 1N HCl at 60 ^{o}C for 2-3 min. to soften the tissue and washed again with distilled water three times. These root tips were then placed on microscopic slides and stained with one drop of acetocarmine solution for 2 minutes. The stained root tips were sealed with cover slip in order to prevent drying[15] and squashed by applying slight pressure to spread the root tip tissues. Three slides were prepared for each concentration including the control (positive and negative). These slides were then observed at 1000 x magnification for cell division and cytogenetic abnormalities. The Mitotic Index (MI) was calculated as the percentage ratio of dividing cells and total number of cells scored (1500) and expressed as percent of negative control.[16] The chromosome aberrations were examined and used as genetic end points for determining cytogenetic effects in inter phase per 1500 cells.[17] The results are expressed as the mean ± SD (standard deviation).

References:

1. A. P. Ginsberg, *Inorganic Synthesis*, John Wiley & Sons, Inc., New york. 1990, **27**, 78.
2. *CrysAlisPro Program*, version 171.37.33c, Agilent Technologies, Oxford, 2012.
3. G. M. Sheldrick, *ActaCrystallogr.*, 2008, **A64**, 112−122.
4. O. V. Dolomanov, L. J. Bourhis, R. J. Gildea, J. A. K. Howard and H. J. Puschmann, *J. Appl. Crystallogr.*, 2009, **42**, 339−341.
5. A. L. Spek, PLATON, *ActaCryst.*, 2009, **D65**, 148-155.
6. V. S. V. Satyanarayana and A. Sivakumar, *Ultrasonics Sonochemistry*, 2011, **18**, 917–922.
7. H. Rajak, R. Deshmukh, R. Veerasamy, A. K. Sharma, P. Mishra and M. D. Kharya, *Bioorg. Med. Chem. Lett.*, 2010, **20**, 4168–4172.
8. S. Goswami and R. Chakrabarty, *Tetrahedron Lett.*, 2009, **50** , 5994–5997.
9. H. Kaur, S. Kumar, P. Vishwakarma, M. Sharma, K. K. Saxena and A. Kumar, *Eur. J. M. Chem.*, 2010, **45**, 2777–2783.
10. C. Allain, S. Favette, L-M. Chamoreau, J. Vaissermann, L. Ruhlmann and B. Hasenknopf, *Eur. J. Inorg. Chem.*, 2008, 3433–3441.
11. P. Yin, C. P. Pradeep, B. Zhang, F.-Y. Li, C. Lydon, M. H. Rosnes, D. Li, E. Bitterlich, L. Xu, L. Cronin and T. Liu, *Chem. Eur. J.*, 2012, **18**, 8157–8162.
12. (a) P. Yin, P. Wu, Z. Xiao, D. Li, E. Bitterlich, J. Zhang, P. Cheng, D. V. Vezenov, T. Liu and Y. Wei, *Angew. Chem.*, 2011, **123**, 2569 –2573; (b) J. Zhang, Y.-F. Song, L. Cronin and T. Liu, *Chem. Eur. J.*, 2010, **16**, 11320 – 11324.
13. (a) J. Rank and M. H. Nielsen, *Hereditas*, 1993, **118**, 49-53; (b) A. S. A. Prasad, V.S.V. Satyanarayana and K.V. B. Rao, *J. Hazard. Mater.*, 2013, **262**, 674– 684.
14. A. K. Sharma, A. Sharma, *Chromosome technique theory and practice*, 3rded., Butterworths, London, UK, 1980, pp. 474.
15. C. B. S. R. Sharma, *Curr. Sci.*, 1983, **52,** 1000–1002.
16. G. Fiskesjo, Allium test for screening chemicals; evaluation of cytologicalparameters, in: W. Wang, J. W. Gorsuch and J. S. Hughes (eds.), Plants and Envi-ronmental Studies., *Lewis Publishers Inc*, New York, NY, 1997, pp. 308–333.
17. A. A. Bakare, A. A. Mosuro and O. Osibanjo, *J. Environ. Biol*, 2000, **21** , 263–271.